

# Journal Pre-proof

Exploring Nanomaterial-modified Biochar for Environmental Remediation Applications

Neda Arabzadeh Nosratabad, Qiangu Yan, Zhiyong Cai, Caixia Wan



PII: S2405-8440(24)13154-4

DOI: <https://doi.org/10.1016/j.heliyon.2024.e37123>

Reference: HLY 37123

To appear in: *HELIYON*

Received Date: 4 March 2024

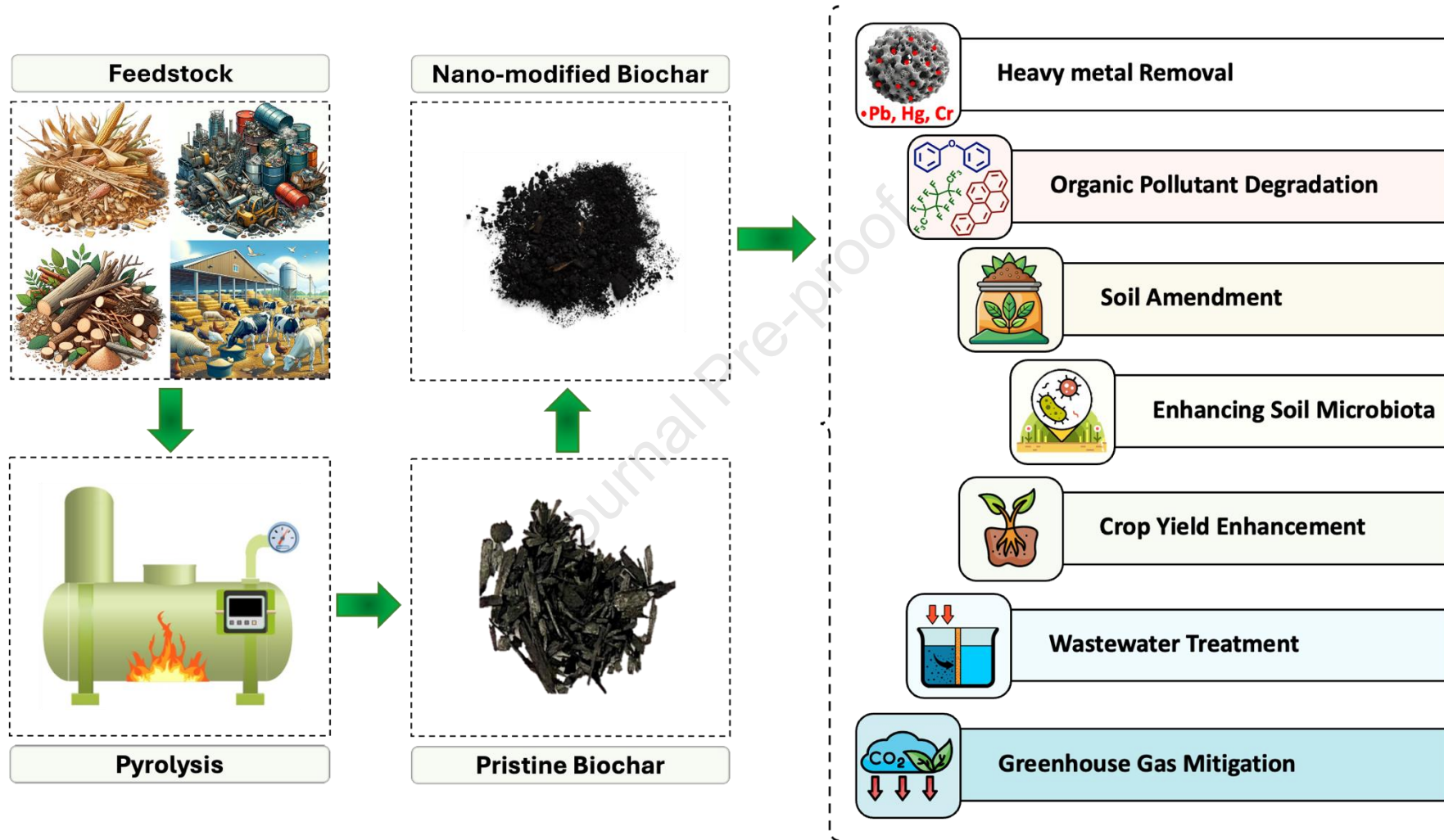
Revised Date: 27 August 2024

Accepted Date: 28 August 2024

Please cite this article as: Exploring Nanomaterial-modified Biochar for Environmental Remediation Applications, *HELIYON*, <https://doi.org/10.1016/j.heliyon.2024.e37123>.

This is a PDF file of an article that has undergone enhancements after acceptance, such as the addition of a cover page and metadata, and formatting for readability, but it is not yet the definitive version of record. This version will undergo additional copyediting, typesetting and review before it is published in its final form, but we are providing this version to give early visibility of the article. Please note that, during the production process, errors may be discovered which could affect the content, and all legal disclaimers that apply to the journal pertain.

© 2024 Published by Elsevier Ltd.



## 1 Exploring Nanomaterial-modified Biochar for Environmental Remediation Applications

2 Neda Arabzadeh Nosratabad <sup>a, †</sup>, Qiangu Yan<sup>b, †</sup>, Zhiyong Cai <sup>b, \*</sup>, Caixia Wan<sup>\*, a</sup>

3 <sup>a</sup> Department of Chemical and Biomedical Engineering, University of Missouri, 1406 East

4 Rollins Street, Columbia, MO 65211

5 <sup>b</sup> Forest Products Laboratory, USDA Forest Service, One Gifford Pinchot Drive, Madison, WI

6 53726-2398

7 <sup>†</sup> These authors contributed equally.

8 <sup>\*</sup> Corresponding author: Email: [zhiyong.cai@usda.gov](mailto:zhiyong.cai@usda.gov) (Zhiyong Cai), Tel: 608-231-9446;

9 [wanca@missouri.edu](mailto:wanca@missouri.edu) (Caixia Wan), Tel: 573-884-7882.

### 10 Abstract

11 Environmental pollution, particularly from heavy metals and toxic elements, poses a  
12 significant threat to both human health and ecological systems. While various remediation  
13 technologies exist, there is an urgent need for cost-effective and sustainable solutions. Biochar, a  
14 carbon-rich product derived from the pyrolysis of organic matters, has emerged as a promising  
15 material for environmental remediation. However, its pristine form has limitations, such as low  
16 adsorption capacities, a relatively narrow range of pH adaptability which can limit its effectiveness  
17 in diverse environmental conditions, and a tendency to lose adsorption capacity rapidly in the  
18 presence of competing ions or organic matters. This review aims to explore the burgeoning field  
19 of nanomaterial-modified biochar, which seeks to overcome the limitations of pristine biochar.  
20 By incorporating nanomaterials, the adsorptive and reactive properties of biochar can be  
21 significantly enhanced. Such modifications, especially biochar supported with metal nanoparticles  
22 (biochar-MNPs), have shown promise in various applications, including the removal of heavy  
23 metals, organic contaminants, and other inorganic pollutants from aqueous environments, soil, and

24 air. This review provides a comprehensive overview of the synthesis techniques, characterization  
25 methods, and applications of biochar-MNPs, as well as discusses their underlying mechanisms for  
26 contaminant removal. It also offers insights into the advantages and challenges of using  
27 nanomaterial-modified biochar for environmental remediation and suggest directions for future  
28 research.

29 **Keywords:** Nanomaterial-modified biochar, biomass, metal nanoparticles, environmental  
30 remediation, nanotechnology

### 31 **1. Introduction**

32 In recent years, there has been growing concerns over the escalating contamination of soil,  
33 water, and air. One of the most pressing concerns is the contamination of soil and water with heavy  
34 metals and toxic elements, such as lead (Pb), arsenic (As), mercury (Hg), and chromium (Cr), in  
35 natural ecosystems [1-7]. These elements are not only highly toxic but also resistant to degradation,  
36 leading to their accumulation in environment. The bioaccumulation of these toxicants can have  
37 detrimental effects on human health, often through the soil-plant-animal-human biological chain  
38 [8]. Air pollution is another critical environmental concern. Driven by industrial activities, vehicle  
39 emissions, and agricultural practices, air pollution introduces a variety of harmful substances into  
40 the atmosphere, including nitrogen oxides (NO<sub>x</sub>), sulfur oxides (SO<sub>x</sub>), volatile organic compounds  
41 (VOCs), and greenhouse gases (GHGs) such as carbon dioxide (CO<sub>2</sub>) and methane (CH<sub>4</sub>) [9].  
42 These pollutants can cause severe health problems, including respiratory and cardiovascular  
43 diseases, and contribute to global climate change [10, 11]. The persistence and bio-accumulative  
44 nature of these contaminants make it imperative to develop effective and sustainable remediation  
45 technologies. For example, remediation of heavy metal-contaminated soil and water has primarily  
46 relied on conventional techniques such as chemical precipitation, ion exchange, and membrane

47 filtration [12]. While these methods have shown some efficacy, they come with their own  
48 challenges, such as use of additional reagents and high membrane costs and membrane fouling.  
49 Micro/nano plastic pollutions further highlight the need for effective remediation strategies to  
50 mitigate environmental and health risks [13].

51 In the context of environmental pollution, biochar has emerged as a promising solution to  
52 various environmental challenges [14]. Biochar is rich in carbon, fine-grained, porous and has  
53 large surface areas. It is produced by pyrolyzing biomass materials, such as plant matters, industrial  
54 byproducts, agricultural waste, sewage sludge, and animal manure, in an environment devoid of  
55 oxygen or with limited oxygen, at temperatures not exceeding 1000 °C, as shown in **Figure 1** [15-  
56 17]. Traditionally used in agriculture as soil amendments, biochar has gained attention for its  
57 multifaceted applications especially for environmental remediation [18, 19]. One of the key  
58 advantages of biochar is its high adsorption capacity, owing to its large specific surface area and  
59 porous structure. These properties make biochar particularly effective for the adsorption of heavy  
60 metals and toxic elements from contaminated soil and water [20]. Biochar is sourced from a variety  
61 of renewable biomass wastes, making it a sustainable and low-cost alternative to other remediation  
62 materials [21, 22]. However, the use of biochar has several challenges. While it offers a cost-  
63 effective and environmentally friendly solution, its efficiency in remediating high-concentration  
64 contaminants has yet to be satisfying. Moreover, the application of large amounts of biochar can  
65 sometimes lead to soil nutrient imbalances, requiring careful consideration of its use in different  
66 environmental settings. Pristine biochar has its own limitations, one of which is its relatively low  
67 adsorption capability for heavy metals and toxic elements. This has led to the exploration of  
68 various modification strategies aiming at enhancing its adsorptive properties. These include  
69 changing surface charges of biochar using metal nanoparticles, expanding its specific surface areas

70 through activating agents, and incorporating metal (or metal oxides) that can interact with  
71 pollutants [23-25].

72         The advent of nanotechnology and the use of nanomaterials have opened new avenues to  
73 enhance the effectiveness of pristine biochar. Incorporating metal nanoparticles (MNPs) into  
74 biochar, resulting in biochar-MNPs, is a promising approach to improve its ability to absorb and  
75 remove contaminants [26, 27]. Nanostructured materials consist of a broad category of substances  
76 that have at least one dimension measuring at the nanometer scale. These materials possess  
77 structural characteristics that fall somewhere between those of bulk solids and molecules. As a  
78 result, they display a unique set of physical, optical, and chemical properties that are distinct from  
79 those of their larger or macroscopic counterparts [28, 29]. By incorporating nanoparticles into the  
80 biochar matrix, researchers have been able to create a material with synergistic properties that far  
81 exceed those of pristine biochar. The nanoparticles serve multiple functions in this hybrid material.  
82 They can increase the surface area and porosity of the biochar, thereby enhancing its adsorption  
83 capacity. Additionally, nanoparticles can introduce new functional groups to the biochar,  
84 increasing its chemical reactivity, and enabling more effective binding with heavy metals and toxic  
85 elements. These nanoparticles, due to their large surface-to-volume ratios compared to the bulk  
86 materials, are highly effective against a wide range of pollutants, especially heavy metals and  
87 organic compounds [30]. However, they tend to clump together into larger particles, reducing their  
88 effectiveness [31]. To address this, biochar has emerged as a popular supporting material for these  
89 nanoparticles, given its high surface area and ion-exchange capacities [32, 33]. Combining biochar  
90 with metal nanoparticles creates a novel composite which maximizes the benefits of both materials  
91 while minimizing their drawbacks. Such composites not only stabilize the nanoparticles but also  
92 enhance their functional properties. Additionally, nanomaterial-modified biochar has the potential

93 to improve air quality by reducing emissions of harmful gases, such as NO<sub>x</sub> and VOCs, through  
94 enhanced adsorption and catalytic processes. Furthermore, it can contribute to mitigating  
95 greenhouse gases by sequestering CO<sub>2</sub> and reducing CH<sub>4</sub> emissions [34]. Biochar's ability to  
96 adsorb air pollutants is influenced by its physiochemical properties, such as surface area and  
97 functional groups, which can be enhanced through various activation processes and pyrolysis  
98 conditions.

99 This review aims to cover the synthesis techniques for biochar-assisted nanomaterials and their  
100 applications in removal of various contaminants from the environment. We also discuss the  
101 mechanisms behind its effectiveness and suggest directions for future research. Additionally, we  
102 explore the potential of these materials to enhance air quality and reduce greenhouse gas emissions,  
103 offering insights into their multifaceted role in environmental remediation and sustainable  
104 practices.

## 105 **2. Nano-modified Biochar Preparation Techniques**

106 Extensive research has been conducted to couple the benefits of biochar's porous structure  
107 with the unique physical attributes of nanomaterials, thereby enhancing its capacity to remove both  
108 organic and inorganic contaminants. Two primary approaches exist for creating nano-modified  
109 biochar with advanced functionalities as depicted in **Figure 2**: one involves modifying the initial  
110 biomass before its conversion into biochar through processes like pyrolysis, calcination, or  
111 coprecipitation; the other one directly alters the already prepared biochar [31, 35-37]. These  
112 modifications often include surface treatments using various metal precursors, nanoparticles, and  
113 organic-inorganic polymers, resulting in biochar nanohybrids. The properties of these biochar-  
114 MNPs are influenced by type of feedstock, pyrolysis temperature, ratio of biochar to metal

115 nanoparticles, and pyrolytic reaction media. The modifications often aim to maximize biochar  
116 yields by optimizing temperature, heating rate, and residence time based on specific feedstock  
117 characteristics [38, 39]. The specific surface area (SSA) values for most nano-modified biochars  
118 range significantly, from 5.58 to 1736 m<sup>2</sup>/g, attributed to their small particle sizes. Research  
119 indicates that nano-modified biochar's SSA can rise with an increase in pyrolysis temperature.  
120 However, there are different views, with some suggesting that an increase in pyrolysis temperature  
121 does not impact or could even decrease the SSA of nano-modified biochars. These discrepancies  
122 could stem from variations in the original materials used to produce the nano-modified biochars  
123 [40]. Enhancing biochar/biochar-MNPs stability involves post-pyrolysis treatments such as  
124 chemical regeneration or physical modification, which not only increase its resistance to  
125 degradation but also its efficacy in environmental applications. Chemical regeneration is a key  
126 method for reactivating biochar, especially for adsorbing heavy metals and organic pollutants like  
127 dyes and antibiotics. The process typically employs solvents and chemical reagents to desorb these  
128 pollutants. The efficiency of regeneration depends on the type of pollutants, and different solvents  
129 are used for organic and inorganic adsorbates. For instance, in a study involving the removal of  
130 lead from wastewater, biochar was regenerated using solutions like sodium hydroxide and  
131 hydrochloric acid. The removal efficiency varied across different cycles, generally showing a  
132 slight decrease in efficiency over successive cycles. This method ensures biochar maintains its  
133 adsorption activity, making it a sustainable option for wastewater treatment [41].

134

## 135 **2.1 Biomass Modification**

136 Biomass pretreatment entails altering raw feedstock before it is converted into biochar  
137 through processes like pyrolysis and calcination. This approach is deemed energy-efficient

138 because it allows for the concurrent processing of both the biomass and metal-containing  
139 precursors. During such alteration processes, the original biomass may be subjected to surface  
140 modifications using a range of metal-containing compounds, specifically metal oxides, metal  
141 chlorides, metal sulfides, metal sulfates, and metal nitrates, along with nanoparticles and organic-  
142 inorganic polymers. These modifications facilitate the creation of biochar-supported  
143 nanomaterials, details of which are elaborated in the following section.

144 Using metal salts to pretreat biomass prior to pyrolysis is a technique for generating  
145 biochar-MNPs. Biomass can be impregnated with various metal salts like  $\text{FeCl}_3$ ,  $\text{Fe}(\text{NO}_3)_3$ ,  $\text{AlCl}_3$ ,  
146  $\text{MgCl}_2$ ,  $\text{MnCl}_2$ ,  $\text{CaCl}_2$ , and  $\text{ZnCl}_2$ , as well as sulfur-based and organic-based metal salt solutions,  
147 either with or without the application of an electric field [42-46]. This allows metal ions in the  
148 solutions to deposit onto the surface or interior of the feedstocks. Following this, the pretreated  
149 biomass undergoes pyrolysis at temperatures ranging from 400 to 800 °C in an environment with  
150 limited or no oxygen. During the pyrolysis process, these metal ions transform into metal oxide  
151 nanoparticles like  $\text{Fe}_2\text{O}_3$ ,  $\text{Al}_2\text{O}_3$ ,  $\text{MgO}$ ,  $\text{MnO}_2$ ,  $\text{CaO}$ , and  $\text{ZnO}$ , or into zero-valent metals that  
152 adhere to the biochar surface. For example, in a study reported by Chaukura et al. [47],  $\text{Fe}_2\text{O}_3$ -  
153 biochar nano-composite was prepared by pyrolyzing  $\text{FeCl}_3$ -impregnated paper and paper sludge  
154 (PPS) at 750 °C. The PPS biomass was immersed in a  $\text{FeCl}_3$  solution for 2 h and then air-dried at  
155 80 °C for another 2 h. The  $\text{FeCl}_3$ -impregnated PPS, with a mass-to-volume ratio of 1:3, was  
156 pyrolyzed at 750 °C for 2 h in a  $\text{N}_2$  atmosphere, yielding  $\text{Fe}_2\text{O}_3$ -biochar. This nanocomposite was  
157 used for the efficient removal of methyl orange (MO) from contaminated wastewater and the  
158 results showed that its MO adsorption capacity was 52.79 % higher than that of pristine biochar.  
159 The surface area and porosity measured by the Brunauer–Emmett–Teller (BET) method were  
160 lower for the  $\text{Fe}_2\text{O}_3$ -biochar composite compared to the pristine biochar. This decrease could be

161 linked to the clogging of the biochar's pores by  $\text{Fe}_2\text{O}_3$  and other inherent metallic compounds in  
162 the absorbent material. Similarly,  $\text{Fe}_3\text{O}_4$ -based magnetic biochar was synthesized by pyrolyzing  
163  $\text{FeCl}_3$ -treated corn straw under an electric field at  $600\text{ }^\circ\text{C}$  for 1 h. This process resulted in the  
164 formation of uniformly dispersed, rod-like  $\text{Fe}_3\text{O}_4$  nanoparticles on the biochar's surface. Notably,  
165 the  $\text{Fe}_3\text{O}_4$ -based magnetic biochar demonstrated a remarkable capacity (113 mg/g) for adsorbing  
166 lead [48]. Bismuth-impregnated biochar was produced through the thermal pyrolysis of bismuth  
167 oxide and hydrochloric acid-treated wheat straw, at temperatures ranging from  $400$  to  $600\text{ }^\circ\text{C}$  [49].  
168 This process, conducted at a heating rate of  $10\text{ }^\circ\text{C}/\text{min}$  in a  $\text{N}_2$  atmosphere for 1 h, resulted in  
169 biochar with a unique porous structure, featuring pores ranging from  $0.5$  to  $1\text{ }\mu\text{m}$  in diameter. This  
170 bismuth-modified biochar was noted for its high capacity in adsorbing phosphorus (125.40 mg/g),  
171 arsenic (16.21 mg/g), and chromium (12.23 mg/g). This study investigated the use of bamboo  
172 biochar, functionalized with Mg-Al and Mg-Fe layered double hydroxides (LDHs), for the  
173 efficient removal of phosphate from aqueous solutions. The composite containing 40% Mg-Al  
174 LDH exhibited the highest phosphate adsorption, achieving over 95% saturation within 1 h. The  
175 research highlighted the potential of using such biochar composites not only for effective  
176 wastewater treatment but also as a recyclable material for agricultural applications, promoting  
177 sustainable environmental management. In another study reported by Omidvar-Hosseini et al.,  
178  $\text{Ni}_{0.5}\text{Zn}_{0.5}\text{Fe}_2\text{O}_4$  magnetic nanoparticles supported on *Acacia Nilotica* seed shell ash (ANSA) were  
179 synthesized and applied for effective adsorption of  $\text{Pb}(\text{II})$  ions from water [50]. An aqueous  
180 mixture of metal nitrates  $\text{Fe}(\text{NO}_3)_3 \cdot 9\text{H}_2\text{O}$ ,  $\text{Zn}(\text{NO}_3)_2 \cdot 6\text{H}_2\text{O}$ ,  $\text{Ni}(\text{NO}_3)_2 \cdot 6\text{H}_2\text{O}$ , and ANSA was  
181 dissolved in DI water, to which extracted egg-white solution was added. Following 30 min of  
182 continuous stirring, the sol-gel obtained was dried at  $80\text{ }^\circ\text{C}$  to yield dry precursors. These  
183 precursors were then finely ground and calcined at  $550\text{ }^\circ\text{C}$  for 2 h in a muffle furnace. Various

184 characterization techniques like Fourier Transform Infrared Spectrometry (FTIR), Scanning  
185 Electron Microscopy (SEM), X-ray Diffraction (XRD), and Vibrating Sample Magnetometer  
186 (VSM) confirmed the successful incorporation of nanoparticles into ANSA, forming less than 100  
187 nm particles with superparamagnetic behavior. The Langmuir model best described the adsorption  
188 process, and the kinetics fit the pseudo-second-order rate equation. The nanoparticles could be  
189 easily separated from water using an external magnet, making them a practical and eco-friendly  
190 solution for treating water pollution caused by Pb (II) ions. Similarly, Li group synthesized nano  
191 ZnO/ZnS-modified biochar via slow pyrolysis of zinc-contaminated corn stover biomass [46].  
192 Slow pyrolysis was conducted in a lab-scale fixed-bed reactor, using zinc-loaded biomass in a  
193 horizontal tubular reactor (60 mm I.D., 300 mm length). The reactor was first purged with N<sub>2</sub> gas  
194 to eliminate O<sub>2</sub>. Biochar from raw corn stover was then produced at four different temperatures:  
195 500, 600, 700, and 800 °C. This modified biochar, uniformly coated with nano ZnO/ZnS, displayed  
196 superior porosity (with a BET surface area of 397.4 m<sup>2</sup>/g and a total pore volume of 0.43 cm<sup>3</sup>/g)  
197 when compared to the unmodified biochar (with a BET surface area of 102.9 m<sup>2</sup>/g and a total pore  
198 volume of 0.20 cm<sup>3</sup>/g). Batch absorption tests indicate that the obtained biochar modified with  
199 nano ZnO/ZnS exhibited a robust ability to absorb Pb (II), Cu (II), and Cr (VI), with maximum  
200 absorption capacities that were notably greater than those of common biochar. Biochar  
201 impregnated with magnesium was prepared by pyrolyzing biomass feedstock (cow dung) and  
202 utilized to reduce the leaching of phosphorus from the soil [51]. The cow dung biomass mixed  
203 with MgCl<sub>2</sub>·6H<sub>2</sub>O solution was placed in porcelain crucibles, which were then sealed and  
204 pyrolyzed at 600 °C for 1 h in an O<sub>2</sub>-limited muffle furnace. This process was aimed at producing  
205 Mg-modified biochar. The data revealed that nanoscale magnesium oxides were uniformly  
206 distributed on the biochar's surface. The MgO-biochar composite had a mesoporous structure with

207 an average pore size of 1.74  $\mu\text{m}$  and could effectively minimize the loss of phosphorus through  
208 leaching from the soil and offer improved stability.

209 Using a low-temperature method, coprecipitation of biomass and metal salts can serve as  
210 another technique for modifying char. A study by Gupta and colleagues introduced a feasible way  
211 to alter the surface of orange peel powder (OPP) by coprecipitating it with ferric chloride  
212 hexahydrate and ferrous sulfate heptahydrate. This led to the creation of a novel magnetic nano-  
213 adsorbent  $\text{Fe}_3\text{O}_4\text{-OPP}$  (MNP-OPP), which showed the covalent binding between the hydroxyl  
214 groups in MNP and the carboxyl groups in OPP. The nanocomposite was further used for cadmium  
215 ion removal from aqueous solutions [52]. It showed that under optimal conditions MNP-OPP  
216 achieved a maximum removal of  $\text{Cd}^{2+}$  at 76.92 mg/g based on Langmuir Model and the adsorption  
217 was thermodynamically favorable.

218 Another approach for creating biochar-MNPs involved directly subjecting biomass rich in  
219 target metal elements to pyrolysis. This process transformed the metal elements in the biomass  
220 into metal nanoparticles. For instance, biochar rich in calcium (CRB) was prepared by carbonizing  
221 crab shells at a temperature ranging from 300 to 900 $^\circ\text{C}$  at a heating rate of 10  $^\circ\text{C}/\text{min}$  for 2 h [53].  
222 Elemental analysis showed a high calcium content, but a low carbon content in the crab shell  
223 biochar. TG indicated that calcite-based CRB was formed at 600  $^\circ\text{C}$ , while lime-based CRB was  
224 generated at 700  $^\circ\text{C}$ . The nanocomposites showed the phosphorus adsorption efficiency varied  
225 from 26% to 100% for a phosphate solution (80 mg/L) and from 11% to 63% for anaerobic  
226 digestion effluent. These findings suggest that CRB was effective for removing or recovering  
227 phosphorus from wastewater.

228 In addition to the use of metal oxides/salts, biochar coated with multi-walled carbon  
229 nanotubes (CNT) were was also reported [54]. Biochar-CNT was produced through slow pyrolysis

230 of carboxyl-functionalized CNT-impregnated feedstocks, including milled hickory chips and  
231 sugarcane bagasse. These CNT-treated feedstocks were placed in a quartz tube within a tubular  
232 furnace (MTI, Richmond, CA) and subjected to pyrolysis at 600 °C for 1 h, with a heating rate of  
233 10 °C/min, in a N<sub>2</sub>-rich environment. It was found that CNTs improved the biochar's  
234 physicochemical attributes, such as surface area, porosity, and thermal stability. Batch sorption  
235 test on methylene blue showed efficient adsorption.

236         Recent studies have increasingly explored the calcination of biomass for biochar and  
237 composite material synthesis. This process involves heating inorganic materials to high  
238 temperatures to improve crystallinity and remove surface impurities and volatiles. An example of  
239 this is the successful synthesis of the sugarcane bagasse-Fe<sub>3</sub>O<sub>4</sub> composite through coprecipitation  
240 of bagasse with FeSO<sub>4</sub>·7H<sub>2</sub>O and FeCl<sub>3</sub>·6H<sub>2</sub>O in the presence of ammonia, followed by calcination  
241 [55]. TEM identified spherical or rod-shaped structures in the altered bagasse. A shift in the IR  
242 spectrum peak from 897 cm<sup>-1</sup> to 874.6 cm<sup>-1</sup> verified the interaction between bagasse and Fe-OH,  
243 while the appearance of Fe-O vibration bands confirmed the composite's formation. Furthermore,  
244 absorption bands at 712.2 cm<sup>-1</sup>, 585.5 cm<sup>-1</sup>, and 436.9 cm<sup>-1</sup> were attributed to Fe-O vibrations, a  
245 consequence of high-temperature calcination.

246         **Table 1** summarizes the various biomass modifications discussed in the section, providing  
247 a comprehensive overview of the feedstocks used, the types of metal precursors involved, the  
248 conditions under which pyrolysis or calcination was carried out, the specific nanocomposites  
249 formed, and their respective applications. This summary table serves as a quick reference for  
250 understanding the diversity of approaches in biomass modification for environmental remediation

251 and pollution control, highlighting the efficiency of each method in creating effective  
252 nanocomposites for targeted applications.

## 253 **2.2 Biochar Modification**

### 254 **2.2.1 Modification Using Metal Precursors**

255 The common approach to acquire biochar-MNPs is enhancing the surface chemistry of  
256 biochar through modification with metal precursors. Initially, biomass undergoes transformation  
257 into biochar through processes like pyrolysis, hydrothermal carbonization, and gasification.  
258 Following this, the biochar is immersed in solutions of metal salts, allowing metal ions to adhere  
259 to the biochar's pores and surface. Ultimately, through processes such as coprecipitation, pyrolysis,  
260 and pH adjustment, metal nanoparticles are deposited onto the biochar's surface, creating biochar-  
261 MNPs. The incorporation of metallic entities into the carbon matrix of biochar not only enhances  
262 its surface properties but also facilitates the easier recovery of the adsorbent material after use. For  
263 instance, manganese dioxide nanoparticles were loaded onto biochar derived from pyrolyzed  
264 invasive water hyacinth using a redox precipitation method, yielding MnO<sub>2</sub>-biochar effective for  
265 the adsorption of Cd (II), Cu (II), Zn (II), and Pb (II) [56]. Compared to biochar alone that showed  
266 negligible adsorption of heavy metal ions, the MnO<sub>2</sub>-biochar nanocomposite demonstrated  
267 substantial capacity for adsorbing these ions. Similarly, the coprecipitation process involving the  
268 ethanol-mediated reduction of KMnO<sub>4</sub> in a biochar suspension led to the creation of the MnO<sub>2</sub>-  
269 biochar nanocomposite with enhanced porosity [57]. The pore volume of this nanocomposite was  
270 approximately three times smaller than that of biochar and 1.5 times smaller than that of nano  
271 MnO<sub>2</sub>. In a study, sewage sludge-derived biochar was first produced by pyrolyzing the sludge at  
272 600 °C for 3 h a 10 °C/min heating rate in a N<sub>2</sub> atmosphere. Subsequently, zero-valent iron

273 nanoparticles were immobilized to the biochar, creating SSB-nZVI-biochar [58]. This composite  
274 showed remarkable efficiency in removing  $\text{Cr}^{6+}$  and  $\text{Pb}^{2+}$  ions from solutions, achieving  
275 approximately 90% and 82% removal within 30 min for  $\text{Cr}^{6+}$  and  $\text{Pb}^{2+}$ , respectively. Kim et al.  
276 modified the Miscanthus biochar with amorphous iron (hydr)oxide to remove arsenite from water  
277 [59]. Miscanthus was initially pyrolyzed at 500 °C for 1 h, using a 10 °C/min heating rate in a  $\text{N}_2$   
278 atmosphere to produce biochar. Then, to prepare Fe-modified biochar, Fe ions were precipitated  
279 onto the biochar by adjusting the pH to 9 using NaOH. This Fe-modified biochar demonstrated  
280 enhanced effectiveness in adsorbing arsenite (56.06 and 47.90 mg/g Fe for powder and beads,  
281 respectively). In their research, Wan et al. utilized bamboo biochar, which was pyrolyzed at 600  
282 °C for 2 h subsequently functionalized with Mg-Al and Mg-Fe layered double hydroxides (LDHs),  
283 to effectively remove phosphate from water solutions [60]. The composite containing 40% Mg-Al  
284 LDH exhibited the highest phosphate adsorption, achieving over 95% saturation within 1 h.  
285 Tomczyk et al. modified sunflower husk biochar with AgNPs for efficient tetracycline removal  
286 [61]. In another study, they effectively created a new electrochemical sensor for the detection of  
287 nitrite, achieved by immobilizing gold nanoparticles to biochar [62]. The resulting biochar/Au  
288 composite displayed distinctive characteristics, including a vast surface area, numerous surface  
289 functional groups, and outstanding conductivity, all contributing to the enhanced performance of  
290 the modified fluorine-doped Titanium oxide electrode in sensing applications. Wang et al.  
291 developed a biochar derived from the seedling of white myoga ginger decorated with gold  
292 nanoparticles (W-biochar/Au) [63]. The as-prepared W-biochar was mixed into the AuNPs  
293 colloidal solution and then subjected to pyrolysis again at a specific temperature (700, 850, or 950  
294 °C) for 2 h. This process resulted in the formation of the W-biochar/Au nanocomposite. The  
295 nanocomposite formed at 850 °C, was employed for the detection of hydroquinone and catechol,

296 demonstrating extremely low detection thresholds and enhanced sensitivities. This nanocomposite  
297 displayed a highly porous configuration, excellent water dispersibility, and an extensive specific  
298 surface area. The notable performance of the W- biochar/Au nanocomposite is likely attributed to  
299 its pronounced porous architecture and increased relative contents of C-O/N-O, C=O, and  
300 COOH/COOR bonds. Zhu et al. developed biochar decorated with magnetic nanoscale zero-valent  
301 iron (nZVI-biochars), featuring varying Fe/biochar impregnation ratios [64]. By systematically  
302 analyzing the mechanisms involved in the removal of heavy metals, they conclusively  
303 demonstrated that nZVI-biochar had superior removal efficiency for various heavy metals ( $\text{Pb}^{2+}$ ,  
304  $\text{Cd}^{2+}$ ,  $\text{Cr}^{6+}$ ,  $\text{Cu}^{2+}$ ,  $\text{Ni}^{2+}$ ,  $\text{Zn}^{2+}$ ). The commendable magnetic properties of the developed material  
305 facilitate the easy recycling of nZVI-biochar from wastewater. In a study by Liao et al., pineapple  
306 peel waste-based biochar is decorated with both magnetic  $\text{Fe}_2\text{O}_3$  and lanthanum hydroxide  
307 ( $\text{La}(\text{OH})_3$ ) and used as phosphate absorbent [65]. As  $\text{La}(\text{OH})_3$  loading in the composite was  
308 increased, the adsorption capacity for phosphate was increased up to 101.16 mg/g although its  
309 magnetic property was reduced. The  $\text{La}(\text{OH})_3$ -modified magnetic biochar had adsorption capacity  
310 27 times greater than the pristine biochar and substantially surpassed most phosphate adsorbents  
311 in capacity. **Table 2** presents a comprehensive overview of modified biochar nanocomposites,  
312 delineating their feedstock sources, metal precursors used for modification, the pyrolysis  
313 techniques employed, and their subsequent applications for environmental remediation.

### 314 2.2.2 Other Modification Techniques

315 Another method of fabrication of biochar involves impregnating biochar with various  
316 organic or inorganic polymers. This impregnation transforms the biochar into an effective  
317 composite, enhancing its porosity and interface chemistry with heavy metal pollutants. For  
318 instance, a bionanocomposite, consisting of an organic-inorganic blend of chitosan, nanoclay, and

319 bark chip-derived biochar, was selected for the simultaneous immobilization of Cu, Pb, and Zn  
320 metal ions in contaminated soil and water environments [66]. This bionanocomposite was prepared  
321 by adding bark chip-derived biochar to the mixture of nanoclay/chitosan solution. The composite  
322 showed a mixed exfoliated/intercalated morphology with the incorporation of minimal nanoclay  
323 amounts (5 wt%). The batch adsorption tests revealed that the nanocomposite's adsorption  
324 capabilities for  $\text{Cu}^{2+}$ ,  $\text{Pb}^{2+}$ , and  $\text{Zn}^{2+}$  significantly surpassed those of the unmodified biochar. As  
325 per the FTIR analysis, the predominant mechanism for metal immobilization is the interaction with  
326  $-\text{NH}_2$  groups. Chitosan was utilized as an organic polymer due to its potential biocompatibility,  
327 environmental friendliness, and its appropriateness for biocomposite preparation [67]. Nanoclay,  
328 with its exchangeable hydrated cations in a layered structure, is commonly applied as an additive  
329 to enhance various physical and adsorptive properties of polymers like chitosan [68].

330 During the preparation of bulk biochar, nanobiochar inherently forms, though its yield is  
331 minimal (e.g.,  $\sim 2.0\%$  in peanut shell biochar).[69] To enhance the nanoparticle content in biochar,  
332 a process for size reduction is essential, which can be conducted effortlessly through grinding or  
333 milling. Prior studies have employed hand grinding with mortars to decrease the size of various  
334 bulk biochars.[70] Ball milling has been underscored as a promising method to boost the yield and  
335 reduce the particle size of nano-modified biochar for large-scale production.[71, 72] Several key  
336 ball milling parameters are ball diameters, mass ratios of balls to biochar, milling speed, duration  
337 of milling, temperature, and liquid media.[73]

338 While nano-modified biochars have demonstrated improved adsorption properties, it is  
339 anticipated that the incorporation of a multi-cationic salt can further enhance adsorption by  
340 introducing a dual adsorption mechanism to the biochar. For example, in a study  $\text{g-C}_3\text{N}_4/\text{FeVO}_4$   
341 (CI) and  $\text{g-C}_3\text{N}_4/\text{FeVO}_4/\text{Fe@NH}_2$ -biochar (CIB) nano-hetero assemblies were synthesized for the

342 removal of methyl paraben (MeP) and 2-chlorophenol (2-CP) using a combination of adsorption  
343 photocatalysis and photo-ozonation [74]. The study demonstrated excellent results, achieving  
344 98.4% degradation of MeP and 90.7% degradation of 2-CP under simultaneous adsorption and  
345 photocatalysis in the presence of CIB. In their research, Wu et al. developed biochar-supported  
346 Ag/Fe nanoparticles (Ag/Fe/MB) for the removal of cephalexin (CLX) in aqueous solution. The  
347 process involved synthesizing nano zerovalent iron (nZVI) with biochar using  $\text{FeSO}_4 \cdot 7\text{H}_2\text{O}$  and  
348  $\text{NaBH}_4$ . This was then treated with  $\text{AgNO}_3$  under vigorous stirring, leading to the formation of a  
349 discontinuous Ag layer on the nZVI/ biochar surface. The Ag/Fe/MB composite was highly  
350 effective in removing CLX from aqueous solution. Specifically, it was found that more than 86%  
351 of CLX was removed by Ag/Fe/MB in 90 min under the conditions of 1.5 g/L Ag/Fe/MB dose,  
352 CLX initial concentration of 20 mg/L, and a pH of 6.15 [75].

353

### 354 **2.3 Characterization of Surface Chemistry and Other Properties**

355 For comprehensive understanding of structural features, physicochemical properties,  
356 contaminant adsorption mechanisms of biochar-MNPs, it is crucial to apply a series of analytical  
357 techniques for extensive characterization as outlined in **Figure 3** and discussed below.

358 FTIR is a powerful tool for the detailed characterization of pristine and nano-modified  
359 biochar biochar, providing insights into their chemical structure, functional groups, and  
360 modifications, which are vital for their applications in environmental remediation and other fields.  
361 For instance, Zhang et al. employed FTIR to reveal numerous surface functional groups of  
362 biochar/Au composite material [62]. The spectral region between  $3500\text{--}3100\text{ cm}^{-1}$  was assigned  
363 to the stretching vibrations of O-H (hydrogen bond). Vibrations of C-H stretching (hydrogen bond)  
364 were represented in the  $3930\text{--}2910\text{ cm}^{-1}$  range. The spectral band from  $1740\text{--}1655\text{ cm}^{-1}$  arose due

365 to the stretching vibrations of C=O. The 1280–1210  $\text{cm}^{-1}$  region corresponded to the stretching of  
366 C-O and the presence of aromatic ring. Lastly, the 1000–650  $\text{cm}^{-1}$  range is associated with  
367 vibrations of M-O, where M denotes metal or Si. Research on studying functional groups on nano-  
368 modified biochars is limited. Biochars are known to have numerous functional groups on their  
369 surfaces and display heterogeneous compositions [69]. The Surface O/C ratios can undergo  
370 substantial modifications, especially at synthesis temperatures between 300-400 °C, impacting the  
371 overall surface behavior, and reactivity [76]. The synthesis temperature is pivotal in determining  
372 the surface characteristics of both bulk and nano-modified biochars. Biochar generated at lower  
373 temperatures (below 400 °C) experiences less severe carbonization and has a lower degree of  
374 aromaticity but more surface functional groups, exhibiting enhanced adsorption capabilities. In  
375 contrast, biochars created at elevated temperatures (higher than 700 °C) tend to have reduced  
376 functional groups due to the removal of heteroatoms like O, N, and S during the charring process  
377 [77]. This leads to the presence of polyaromatic rings (characterized by X-ray adsorption  
378 spectroscopy) with various functional groups such as O-, S-, and N-functional entities. The  
379 hydrophilic properties and negative charges are predominantly attributed to the O-functional  
380 groups such as -OH, -COOH, -C=O, and -C-O, as the deprotonation of these groups results in  
381 net negative surfaces [78]. Additionally, nano-modified biochars may incorporate N-H bonds and  
382 SiO<sub>2</sub>. Comparatively, nano-modified biochars feature both polar and non-polar sites along with a  
383 plethora of hydroxyl, carboxylic, and carbonyl functional groups.

384 BET method is utilized to ascertain specific surface area and distribution of pore sizes. For  
385 example, Zhang et al. used BET surface analyzer to measure the pore size distribution and surface  
386 area of biochar-MnO<sub>2</sub> material [56]. Biochar initially had a minimal BET surface area of 3.5  $\text{m}^2/\text{g}$   
387 due to its substantial particle size. However, a notable enhancement in its BET surface area was

388 observed upon the deposition of MnO<sub>2</sub>. Biochar loaded with varying amounts of MnO<sub>2</sub> displayed  
389 superior specific surface areas compared to unmodified biochar, indicating the augmentation in  
390 biochar's specific surface area via post-MnO<sub>2</sub> modification. The specific surface area of biochar-  
391 MnO<sub>2</sub> escalated from 135.9 m<sup>2</sup>/g to 181.5 m<sup>2</sup>/g as the MnO<sub>2</sub> loading amount rose from 12.3% to  
392 18.4%. Conversely, a further increase in MnO<sub>2</sub> loading amount resulted in a decline in the specific  
393 surface area of biochar-MnO<sub>2</sub>. The initial enhancement can be attributed to the incorporation of  
394 MnO<sub>2</sub> nanoparticles and the formation of additional micropores. The subsequent reduction at  
395 elevated loading is presumably due to the excessive deposition of MnO<sub>2</sub> nanoparticles, potentially  
396 causing blockage of pores and disruption of certain micropore structures.

397 Transmission Electron Microscopy (TEM) and SEM are employed to examine the  
398 microstructure, morphology, and the dispersion of metal nanoparticles within biochar-MNPs. For  
399 instance, Yang et al. explored the structure and morphology of the biochar/Fe-Mn-S composite  
400 utilizing SEM and TEM [79]. SEM imagery revealed that the ternary needle-like Fe-Mn-S  
401 mixtures were uniformly distributed on the hierarchical biochar, which possessed numerous  
402 regular and vertical channels. TEM images displayed the contours of nanorods, having diameters  
403 of several nanometers and lengths varying from several to hundreds of nanometers. Energy-  
404 Dispersive X-ray Spectroscopy (EDS) is a technique used for characterizing the elemental  
405 composition of materials. If biochar is modified with metal nanoparticles, EDS can confirm the  
406 presence of metal elements on the biochar surface and provide information about their  
407 concentration and distribution. Wang group adopted EDS to analyze the types and molar fraction  
408 of elements in a biochar sample decorated with gold nanoparticles [80]. The distributions of C, O,  
409 N, and Au appear to be uniform across the entire surface. Therefore, the combined results from  
410 their SEM and EDS analyses effectively demonstrate the embellishment of biochar with gold

411 nanoparticles. In addition, elemental analyzer was also used for analyzing C, H, O, and N. Biochar  
412 is predominantly composed of those elements, along with varying concentrations of vital mineral  
413 nutrients, and exhibit significant diversity in trace elements. The nitrogen component of biochar is  
414 influenced by feedstock and pyrolysis temperature as peptide bonds transform into N-  
415 heteroaromatic carbon compounds [69]. Biochar derived from plants usually possesses a richer  
416 mineral content.

417 XRD is a versatile tool that can provide a wealth of information about the structural and  
418 compositional characteristics of pristine and nano-modified biochars . It can provide valuable  
419 insights into the crystalline nature, mineral content, and other structural attributes of the char by  
420 analyzing the diffraction patterns. For instance, Wang et al. employed XRD to examine the  
421 crystalline phase and structural characteristics of magnetic nano-modified biochar [81]. The XRD  
422 analysis of the magnetic nano-modified biochar revealed peaks at  $2\theta$  values of  $30.2^\circ$ ,  $35.6^\circ$ ,  $43.3^\circ$ ,  
423  $53.7^\circ$ ,  $57.2^\circ$ , and  $62.9^\circ$ , which correspond to the  $\gamma\text{-Fe}_2\text{O}_3$  crystalline phases. Given the similar  
424 diffraction peaks of  $\gamma\text{-Fe}_2\text{O}_3$  and  $\text{Fe}_3\text{O}_4$ , the XRD results confirmed the formation of both  $\text{Fe}_3\text{O}_4$   
425 particles within the composite.

426 X-ray Photoelectron Spectroscopy (XPS) is a surface-sensitive analytical technique that  
427 provides information about the elemental composition, chemical state, and electronic state of the  
428 elements present in the pristine and nano-modified biochars . In 2019, Yang group utilized XPS  
429 to examine the surface composition and chemical states of a straw biochar functionalized with  
430 lanthanum ferrite ( $\text{LaFeO}_3$ ) nanoparticles [82]. The observed peaks at 835.0, 836.2, and 839.7 eV  
431 for  $\text{LaFeO}_3/\text{biochar}$  correspond to the binding energies of La (3d), suggesting that La is  
432 predominantly in its oxidized state. For  $\text{LaFeO}_3/\text{biochar}$ , the Fe (2p) peaks are located at 711.5 and  
433 725.1 eV, with no discernible shoulder peaks, signifying the Fe ions are in the  $\text{Fe}^{3+}$  oxidation state.

434 The 529.8 eV peak is attributed to lattice oxygen atoms, specifically La–O and Fe–O in the LaFeO<sub>3</sub>  
435 crystal structure. Regarding C in LaFeO<sub>3</sub>/biochar, the C (1s) signal deconvolution revealed the  
436 presence of C–C bonds at binding energies of 283.7, 284.7, and 285.1 eV. This data confirms the  
437 successful incorporation of LaFeO<sub>3</sub> onto the biochar surface.

438 Thermogravimetric Analysis (TGA) is a thermal analysis technique used to measure the  
439 weight change of a sample as a function of temperature or time under a controlled atmosphere. For  
440 example, Zhang et al. employed TGA to study the development of MgO-biochar [83]. The TGA  
441 curve for sugar beet tailings revealed four distinct weight loss phases. The first phase, from 30 to  
442 200 °C, was due to residual water molecule evaporation. The subsequent phases, from 200 to 300  
443 °C, 300 to 400 °C, and 400 to 550 °C, were attributed to the decomposition of lignin, cellulose,  
444 and hemicellulose, respectively. The TGA curve for MgCl<sub>2</sub>-treated sugar beet tailings also showed  
445 four stages. The initial weight loss was due to the water molecule evaporation from 30 to 100 °C.  
446 The subsequent decrease in weight was linked to the breakdown of MgCl<sub>2</sub> hydrates from 100 to  
447 250 °C. The third drop in weight was likely due to the formation of magnesium hydroxychloride  
448 and the further degradation of hydrates from 250 to 450 °C. The final weight reduction was  
449 associated with magnesium oxide formation alongside decomposition of magnesium  
450 hydroxychloride from 450 to 650 °C.

451 VSM provides a comprehensive analysis of the magnetic properties of pristine and nano-  
452 modified biochars. For example, Li et al. utilized a vibrating sample magnetometer to assess the  
453 magnetic saturation of biochar fabricated with magnesium oxide [84]. The biochar impregnated  
454 with magnesium displayed a saturation magnetization of 35.35 emu/g, suggesting it could be  
455 readily magnetized. Impressively, even after being submerged in water for five months, this

456 magnesium-impregnated magnetic biochar could be effectively recaptured using a permanent  
457 magnet.

458 In recent years, innovative methods have been employed to analyze multifunctional  
459 composites. Techniques like X-ray Absorption Near-Edge Structure (XANES) and extended X-  
460 ray Absorption Fine Structure (EXAFS) are used to provide deep insights into the interaction  
461 between the biochar matrix and the nanoparticles, the chemical state of the metals, and the nature  
462 of the metal-containing species. Confocal Micro X-ray Fluorescence ( $\mu$ -XRF) is applied to  
463 ascertain the elemental composition and distribution in biochar-MNPs [85]. In a study by Feng et  
464 al. they utilized XANES, EXAFS, and  $\mu$ -XRF to study the characteristics of Fe-biochar [86]. The  
465 results from Fe XANES and EXAFS revealed  $\gamma$ -Fe<sub>2</sub>O<sub>3</sub> as the dominant Fe species in the composite,  
466 with Fe<sup>0</sup> being detected at temperatures of 600 or 900 °C. The  $\mu$ -XRF analysis highlighted the  
467 dispersion of Fe, S, and Cl within the porous structure, with Fe accumulating on the biochar's  
468 surface.

### 469 **3. Multifunctional Applications of Nano-modified Biochar in Environmental Remediation**

470 Recent studies have delved into nano-modified biochars' diverse applications, such as  
471 catalyst, alternative for carbon black, biomolecule carrier, and the removal of various contaminants  
472 like agrochemicals and pharmaceuticals [73, 87-89]. Due to its superior adsorptive properties,  
473 nano-modified biochar showcases an impressive ability to adsorb a broad spectrum of  
474 contaminants. Moreover, nano-modified biochar can also act as a catalyst, promoting the  
475 decomposition of organic compounds [90].

#### 476 **3.1 Heavy Metal Removal**

477 Heavy metal contamination poses significant environmental threats, impacting both  
478 ecosystems and public health. Nano-modified biochar have gained prominence due to its notable  
479 reactivity, high surface area, and ion-exchange capabilities, making it effective in addressing heavy  
480 metals like As, Hg, Cr, Cu, Cd, and Pb [91]. Some of these heavy metals are non-essential and  
481 known to be detrimental to human health due to their acute and chronic toxic effects. Meanwhile,  
482 others are trace elements vital for human well-being but can become harmful if their levels surpass  
483 the recommended thresholds [92]. Therefore, effective heavy metal removal strategies including  
484 stabilization, microbial remediation, and electrochemical methods, are required in agricultural and  
485 environmental research. Several factors, including dosage, presence of other ions, initial heavy  
486 metal concentration, and pH, influence nano-modified biochar's performance. The removal  
487 processes involve multiple mechanisms, including adsorption, reduction, precipitation, co-  
488 precipitation, ion exchange, and oxidation. To elucidate these mechanisms, various analytical  
489 techniques as shown in **Figure 3** are employed. The ability of nano-modified biochars to extract  
490 heavy metals, the influence of different factors on this removal efficiency, and the underlying  
491 mechanisms are comprehensively discussed below.

492 Numerous studies have demonstrated the effectiveness of nano-modified biochars in  
493 removing heavy metals and have assessed its capacity for such removal. To gauge the efficiency  
494 of nano-modified biochars in extracting heavy metals, various models such as Langmuir,  
495 Freundlich, Langmuir-Freundlich, Temkin, and Sips are used to interpret the collected data.  
496 Moreover, models like the first-order kinetic, Elovich, intraparticle diffusion, and second-order  
497 kinetic are applied to ascertain the rate of heavy metal removal. In a study by Wan et al., a magnetic  
498 biochar, which combines the advantages of both biochar and iron oxides, effectively removed  
499 multiple metal(loid) contaminants from the soil [93]. There was a notable reduction in the soil

500 concentrations of As, Cd, and Pb by 28%, 25%, and 32%, respectively, within 24 h. The Fe<sub>3</sub>O<sub>4</sub>-  
501 modified biochar not only removed the soluble and exchangeable fractions of metal(loid)s but also  
502 directly adsorbed the solid fractions. A novel porous biochar activated with K<sub>2</sub>CO<sub>3</sub> and infused  
503 with nano-zero-valent iron and nano- $\alpha$ -hydroxy-iron oxide was tested for Cd (II) removal from  
504 aqueous solution, as reported by Zhu et al [94]. The Cd (II) adsorption onto this composite was  
505 best explained by the pseudo second-order kinetic model, suggesting that chemisorption primarily  
506 controlled the process. The composite's adsorption rates for Cd (II) were notably rapid.  
507 Furthermore, the Langmuir model provided the most accurate fit for the experimental data. The  
508 composites' maximum adsorption capacities for Cd (II) were measured at 26.43 mg/g and 22.37  
509 mg/g. When compared to other materials, these composites demonstrated superior efficacy in  
510 removing Cd (II). Nano-modified biochar prepared by ball-milling process was used to remove Ni  
511 (II) (a model contaminant).[73] The results showed that this ball-milled nano-modified biochar  
512 was more efficient in Ni (II) removal than the pristine biochar. It also demonstrated rapid  
513 adsorption rates and outstanding Ni (II) absorption capacity, surpassing many commercial sorbents  
514 (e.g., Activated carbon, Na-montmorillonite, natural bentonite, and *Chlorella sorokiniana*).  
515 Compared to the pristine biochar, the ball-milled nano-modified biochar exhibited enhanced  
516 physical and chemical features, such as increased surface areas and more acidic functional groups.  
517 As a result, its ability to remove contaminants surpassed that of the pristine biochar.

518         The effectiveness and stability of heavy metal removal using nano-modified biochars  
519 depend on various environmental factors (soil minerals, feedstock, pyrolysis temperature,  
520 nanoparticle content, biochar loading, additives, etc.). For instance, when using biochar loaded  
521 with polymetallic nanoparticles, the heavy metal immobilization varies based on the nanoparticle  
522 to biochar ratio. In a study reported by Zhang et al., they examined how the addition of iron,

523 manganese, and cerium oxide (FMCBC) to biochar affected arsenic availability in arsenic-polluted  
524 paddy soil [95]. The FMCBC with different mass ratios of 24:2:3:4 (FMCBC<sub>1</sub>), 24:2:3:8  
525 (FMCBC<sub>2</sub>), and 24:2:3:10 (FMCBC<sub>3</sub>) for biochar, Fe, Mn, and Ce respectively, is used for the  
526 polluted soil treatment. The findings indicate that FMCBCs enhance the soil's pH and redox  
527 potential, leading to a reduction in the bioavailable arsenic forms. Among all treatments, FMCBC<sub>3</sub>  
528 had the highest reduction in soil-bound arsenic concentration. The conditions under which  
529 pyrolysis is conducted, including temperature and gas flow, influence the functional groups and  
530 surface area of biochar composites. For example, greater immobilization of Cr is observed at  
531 higher pyrolysis temperatures, specifically at 700 °, as noted by Rafique et al [96]. As pyrolysis  
532 temperatures rise, groups like alcoholic, aliphatic, and ester on the biochar surface diminish, as  
533 observed by Shakya et al [97]. Additionally, hemicellulose breaks down at temperatures above  
534 350 °C, leading to a rapid release of volatile compounds that form pores [98]. As a result, the  
535 capacity to immobilize increases with temperature due to enhanced surface area.

### 536 **3.2 Organic Pollutant Removal**

537 Nano-modified biochars also demonstrated a strong adsorption to organic contaminants.  
538 Nano-modified biochar serves as an adsorbent, reductant, and catalyst in removing organic  
539 contaminants such as persistent organic pollutants, cancer-causing compounds, pesticides, and  
540 antibiotics. This is applied to environmental and agricultural settings because of its strong  
541 adsorptive, catalytic, and reductive properties. Recent research indicates that carcinogenic  
542 persistent organic pollutants (POPs), such as polycyclic aromatic hydrocarbons (PAHs) and  
543 polybrominated diphenyl ethers (PBDEs), can make their way to the food chain. Due to their  
544 carcinogenic properties (e.g., low solubility, high molecular weight, and persistence), they pose  
545 potential threats to both human health and the environment [99, 100]. Therefore, nano-modified

546 biochars can serve as an effective tool for removing these pollutants from the environment. For  
547 instance, using the liquid phase reduction method, biochar-supported nano zero-valent iron  
548 (biochar-nZVI) was synthesized to activate persulfate (PS) for decabromodiphenyl ether  
549 (BDE209) removal from soil [101]. The data indicated that at a PS/biochar-nZVI molar ratio of  
550 3:1, pH 3, and 40 °C, 82.06% reduction of BDE209 was achieved in 4 h. In another study, biochar  
551 nanocomposites modified with copper oxide (CuO) were synthesized for removing anionic  
552 contaminants (reactive red RR120) from water [102]. The work highlighted the robust interaction  
553 between CuO and biochar. The embedded CuO nanoparticles in the composite demonstrated  
554 superior removal of reactive red due to strong electrostatic attraction. The CuO/biochar  
555 nanocomposite showcased the best RR120 removal efficiency at 46%, significantly outperforming  
556 the original biochar at 20%. Furthermore, the adsorption process was quick, with an equilibrium  
557 time of less than 3 h. The impact of different particle sizes (sub-millimeter, micron-scale, and  
558 nano-scale) of biochar derived from corn straw and rice husk was studied on the adsorption of  
559 diethyl phthalate (DEP) [103]. The findings revealed that the smaller the biochar particle size, the  
560 greater its capacity to adsorb DEP, with nano-scale biochar demonstrating the highest adsorption  
561 capability. This increased adsorption in nano-scale biochar was due to its advanced pore structure  
562 and larger specific surface area. This suggests that nano-scale biochar's DEP adsorption primarily  
563 resulted from pore-filling, rather than interactions like  $\pi$ - $\pi$  EDA and H bonding observed in larger-  
564 sized biochar. Moreover, the nano-scale biochar's ability to adsorb DEP significantly dropped  
565 when the initial pH value was reduced from 9 to 3. This was because an acidic environment  
566 diminished the surface charge on the nano-scale biochar, causing easier agglomeration of the  
567 particles. Phthalate esters (PAEs) are commonly used as plasticizers in plastic products worldwide,  
568 leading to the potential bioaccumulation of benzene carboxylic groups. It is crucial to remove

569 PAEs from environments like soil and sediment. Two prominent plasticizers, Dibutyl phthalate  
570 (DBP) and di-(2-Ethylhexyl) phthalate (DEHP), are prevalent residues in soil and are listed as  
571 priority pollutants by the US Environmental Protection Agency. In a study, the impact of using the  
572 Fe-Mn oxide-modified biochar composite (FM-biochar) was investigated on the quality of wheat  
573 cultivated in brown soil contaminated with DBP and DEHP [104]. Introducing FM-biochar notably  
574 reduced the absorption of DBP and DEHP by wheat grains, leading to enhancements in the grain  
575 quality, specifically in starch, protein, and amino acid levels. Moreover, the results from FM-  
576 biochar applications surpassed those from biochar treatments, suggesting that FM-biochar is a  
577 potent method to lower the bioavailability of PAEs to wheat grains. In their report Bentley et al.  
578 showed improved adsorption capacities for certain organic micropollutants (OMPs) using pine-  
579 derived biochars pre-treated with NaOH (pH 9 and 11) and various alkali and alkaline earth metals  
580 (AAEMs) like Na, K, Ca, and Mg [105]. This treatment notably increased the surface area of the  
581 biochar's micropores, with the most significant improvement observed at pH 11, where the OMP  
582 adsorption rate nearly matched that of commercial activated carbon, surpassing untreated biochars.  
583 This underscores the effectiveness of specific pre-treatments in enhancing biochar for water  
584 treatment applications.

### 585 **3.3 Nano-modified Biochars' Role in Soil Health and Air Quality**

586 Biochars, as soil amendments, have a significant impact on soil microbial activity, playing  
587 a crucial role in enhancing soil health and fertility. Their porous structure and high surface area  
588 provide a conducive habitat for diverse microbial communities, facilitating the proliferation of  
589 beneficial microorganisms. Biochars are known to influence soil pH, moisture retention, and  
590 nutrient availability, all of which are critical factors affecting microbial growth and activity.  
591 Notably, they can improve the soil's carbon content, offering a stable carbon source for soil

592 microbes, thus stimulating their metabolic processes. The interaction between biochar and soil  
593 microbes often leads to increased soil enzyme activities, indicative of enhanced nutrient cycling  
594 and organic matter decomposition. Furthermore, the presence of biochar can help in mitigating the  
595 negative effects of soil contaminants, thereby reducing the stress on microbial communities. This,  
596 in turn, supports the restoration of microbial diversity and function in degraded soils.

597         Soil microorganisms play a pivotal role in nutrient cycling, breaking down soil organic  
598 matter to release nutrients in accessible forms for plants and other microbes, integral to the soil-  
599 plant biogeochemical cycle. Any changes affecting these microbes or nutrient cycling can impact  
600 ecosystem functionality. Previous findings indicate that nano-modified biochars can transform the  
601 composition of soil microbial communities and influence their metabolic capacity, particularly in  
602 nutrient cycles like carbon and nitrogen cycling. The presence of nano-modified biochars affects  
603 enzyme activities, functional genes, and microbial species involved in nitrogen and carbon cycling.  
604 Factors such as soil pH, bioavailable metals, and soil electric conductivity (EC) also impact  
605 bacterial communities, hindering phototroph growth and leading to a decrease in carbon fixation  
606 genes [106]. Additionally, dissolved organic carbon (DOC) released from biochar forms reactive  
607 oxygen species, which can damage cellular components of phototrophs, reducing the relative  
608 abundance of carbon fixation genes [107]. The promotion of carbon-degrading organisms by  
609 MgO-biochar might be associated with increased cellulase activity, releasing more glucose and  
610 thereby boosting the abundance of carbon-utilizing bacteria [108]. In some cases, the rise in certain  
611 key orders related to carbon-cycling bacteria in modified biochar treatments could regulate the  
612 carbon cycle. In general, the use of nano-modified biochars can influence crop growth and yield,  
613 affect the behavior and survival of soil fauna, and alter soil properties like pH and organic matter

614 [109]. These changes impact the structure of soil microbial communities, which are crucial for  
615 processes like carbon and nitrogen cycling.

616 Nano-modified biochars have also shown significant potential in improving air quality by  
617 reducing emissions of harmful gases such as nitrous oxide ( $\text{N}_2\text{O}$ ) and methane ( $\text{CH}_4$ ), and  
618 sequestering greenhouse gases like carbon dioxide ( $\text{CO}_2$ ) [110-112]. The high surface area and  
619 reactivity of nano-modified biochar enable it to adsorb pollutants more efficiently than  
620 conventional biochar. By altering the soil's physicochemical properties, nano-modified biochar  
621 enhances its ability to retain and degrade airborne pollutants and provides a more favorable  
622 environment for microbial communities that break down these gases. This, in turn, contributes to  
623 both improved soil health and air quality by decreasing greenhouse gas emissions through the  
624 modification of soil microbial activities that influence the nitrogen and carbon cycles [34].

#### 625 **4. Mechanisms of Pollutant Removal by Nano-modified Biochars**

626 As discussed above, nano-modified biochar has been identified as a capable adsorbent  
627 for removing specific pollutants, including heavy metals and organic pollutants. Understanding  
628 the interaction mechanism between pollutants and nano-modified biochar is vital for linking  
629 remediation to the engineering design of these materials [113, 114]. Factors such as pH and  
630 material dosage significantly influence the efficiency of dissipation. Extensive research has been  
631 carried out to explore the remediation abilities of nano-modified biochar for heavy metals and  
632 organic compounds in polluted environments. The proposed mechanisms behind pollutant  
633 adsorption are illustrated in **Figure 4** and discussed below.

#### 634 **4.1 Mechanisms Involved in Metal Removal**

635 *Electrostatic Interactions.* Electrostatic adsorption, which is fundamental to the formation  
636 of ionic bonds, can be affected by factors such as point of zero charge (PZC), the pH level, and the

637 heavy metal's ionic and valence radii. In general, elements like chromium, arsenic, and antimony  
638 form anionic species in water, and because they are negatively charged, they tend to repel away  
639 from the similarly charged surface of unmodified biochar. This electrostatic repulsion limits the  
640 capacity of pristine biochar to adsorb these elements. To overcome this limitation, modifications  
641 to biochar are often employed to improve its adsorption capabilities. For example, Zhang et al.  
642 observed that by loading chitosan into bamboo biochar, the adsorption capacity for hexavalent  
643 chromium (Cr(VI)) was significantly enhanced, reaching up to 127 mg/g of biochar. This increase  
644 in adsorption was attributed to the electrostatic attraction between the positively charged hydroxyl  
645 and amine groups of chitosan and the  $\text{CrO}_4^{2-}$  ions [115]. Likewise, it was reported that the KOH-  
646 modified, nitrogen-enriched biochar (KNB) derived from waste chicken feathers, was effectively  
647 utilized for the adsorption of Cd and Pb from wastewater [116]. KOH modification significantly  
648 enhanced the adsorption capacities of the biochar. Electrostatic interactions were one of the  
649 primary mechanisms for Cd and Pb adsorption by KNB. The modification with KOH enhanced  
650 the biochar's surface functional groups, which in turn increased its electronegativity. This  
651 enhancement led to a stronger electrostatic attraction to Cd and Pb ions.

652         The adsorption efficiency of engineered biochar for positively charged heavy metals, such  
653 as cadmium, lead, copper, zinc, and nickel, is significantly affected by several factors. These  
654 factors include the surface area of biochar, its zeta potential, the nature of minerals present in  
655 biochar, the types of functional groups on the biochar surface, as well as the conditions present in  
656 the solution. For example, FTIR analysis indicated that  $\text{Cd}^{2+}$  ions were likely adsorbed onto the  
657 surface of iron oxide through electrostatic attraction. Furthermore, the analysis suggested that  
658 surface complexation occurs between the  $\text{Cd}^{2+}$  ions and the  $\text{Fe}_3\text{O}_4$ , involving  $\pi$ -orbital bonding of  
659 the metal ions to the  $\pi$ -electrons of the carbon atoms on the surface [117].

660           **Complexation.** The surfaces of biochar are enriched with oxygen-containing functional  
661 groups such as -OH, -COH, and -COOH. These groups participate in complex formation with  
662 metal ions, resulting in the creation of stable metal complexes. For instance, a biochar supported  
663 nano-scale zero-valent iron (biochar-CMC-nZVI), which was stabilized with carboxymethyl  
664 cellulose (CMC), was utilized for the effective removal of hexavalent chromium (Cr (VI)) from  
665 water [118]. The XPS pattern indicated that alcohol, phenolic, aliphatic, and aromatic carbon were  
666 present, suggesting that surface complexation played a crucial role in the adsorption process of  
667 Cr(VI). The FTIR spectra of the composite post-reaction revealed alterations in the Fe-O, C-O,  
668 and O-C=O groups, indicating that complexation and electrostatic attraction occurred between Cr  
669 (VI) and the composite's iron-containing functional groups. Also, various materials such as metal  
670 oxides, sulfides, and carbon-based nanomaterials have been utilized to enhance biochar for the  
671 purpose of extracting Sb from water [119, 120]. In a specific instance, Wang et al. developed  
672 biochar infused with lanthanum (La) that possessed magnetic properties [121]. This modification  
673 significantly boosted its capacity to adsorb Sb(V), with the adsorption capacity rising from 2.2 to  
674 18.9 mg/g at a neutral pH of 7. Characterization using FTIR and XPS techniques indicated that the  
675 primary mechanism behind the improved adsorption of Sb(V) was the formation of a stable inner-  
676 sphere La-O-Sb complex within the material's structure.

677           **Ion Exchange.** Ion exchange involved the selective exchange of exchangeable metal ions  
678 like  $K^+$ ,  $Mg^{2+}$ ,  $Na^+$ , and  $Ca^{2+}$  on the biochar surface with other metal ions. This process is largely  
679 influenced by the chemical characteristics of the biochar's surface [122]. The investigation into the  
680 mechanism behind Cu (II) removal by  $Fe_3O_4$ -alginate modified biochar involved characterizing  
681 the composite post Cu (II) adsorption using FTIR and XPS techniques [123]. Shifts and changes  
682 in the FTIR spectral adsorption peaks after Cu (II) adsorption suggested interactions between Cu

683 (II) and the composite's functional groups. Moreover, notable shifts in the Cu 2p and Fe 2p peaks  
684 in the XPS spectrum regarding post Cu (II) adsorption indicated that ion exchange took place  
685 between Cu (II), the composite material, and Fe<sub>3</sub>O<sub>4</sub>.

686 **Redox Reactions.** Some biochars may facilitate redox reactions due to the presence of  
687 electron-donating or accepting sites. This can transform the metal ions into a less mobile and less  
688 toxic state [124]. For example, an iron-enhanced biochar, was utilized to assess the absorption  
689 capacity of As, Cd, and Pb by rice crops. Heavy metals, particularly arsenic in the forms of As  
690 (III) and As (V), undergo redox reactions on the surface of biochar due to the strong oxidizing and  
691 reducing agents present, resulting in the formation of stable inner-sphere complexation of As on  
692 the biochar surface [125].

693 **Precipitation.** Biochar can co-precipitate with heavy metal cations, forming insoluble  
694 carbonates and phosphates that serve to immobilize heavy metals in soils. Liang et al. enhanced  
695 biochar derived from glucose by activating it with KOH and incorporating nitrogen at a pyrolysis  
696 temperature of 800 °C [126]. This modification endowed the biochar with a substantial Cr (VI)  
697 adsorption capability of 402.9 mg/g. The adsorption process involved a combination of  
698 mechanisms, including physical adsorption, electrostatic attraction, surface complexation, and the  
699 reduction of Cr (VI) to Cr (III), followed by the adsorption and precipitation of the reduced Cr (III)  
700 species.

701 Other mechanisms like physical adsorption and micropore filling can also be involved in  
702 heavy metal removal. The porous nature of biochar provides a large surface area that facilitates  
703 the physical adsorption of metal ions. This is a non-specific process where metal ions are retained  
704 on the surface of biochar through van der Waals forces [122]. In the micropore filling, heavy metal

705 ions may get trapped within the micropores of the biochar, especially if the pore size is compatible  
706 with the size of the metal ions.

#### 707 **4.2 Mechanisms involved in organic pollutant removal**

708 Organic pollutants such as dyes, pesticides, antibiotics, plasticizers, PAHs, and phenols  
709 represent significant categories of contaminants in the environment. The primary removal  
710 mechanisms for these common organic pollutants by nano-modified biochars are depicted in  
711 **Figure 4**. The adsorption of organic contaminants on biochar is controlled by several mechanisms,  
712 predominantly including pore-filling,  $\pi$ - $\pi$  interactions, hydrophobic effects, electrostatic  
713 attraction, and hydrogen bonding as discussed below.

714 **Pore Filling.** The process of pore-filling plays a crucial role in the adsorption of organic  
715 substances onto biochar. The capacity for adsorption is directly proportional to the surface area of  
716 the micropores [127]. Chen et al., discovered that the surface area of biochar, which affects the  
717 absorption rate of naphthalene (NAP) in solutions, is determined by the temperature at which the  
718 biochar is pyrolyzed [128]. Higher pyrolysis temperatures lead to more complete carbonization of  
719 the organic components in the biomass, resulting in biochar with a greater degree of carbonization,  
720 a larger surface area, and more developed micropores, all of which contribute to a higher sorption  
721 rate. Zhu et al. also noted that the extensive surface area and pore volume of carbon-based materials  
722 typically enhance the sorption of organic pollutants due to the pore-filling effect [129].

723  **$\pi$ - $\pi$  Interactions.** Many organic pollutants have aromatic components that can undergo  $\pi$ -  
724  $\pi$  electron donor-acceptor interactions with aromatic regions in biochar. Xie et al. reported a strong  
725 correlation between the adsorption of sulfonamides (SAs) and the degree of graphitization of  
726 various biochars [130]. They attributed this correlation to the  $\pi$ - $\pi$  electron donor-acceptor (EDA)  
727 interactions that occur between the graphitic surfaces of the biochars (which act as  $\pi$  electron

728 donors) and the SAs (which act as  $\pi$  electron acceptors), leading to the pronounced adsorption  
729 observed. In a different study, a graphene oxide-modified magnetic sludge biochar (GO/CoFe<sub>2</sub>O<sub>4</sub>-  
730 S biochar) was developed for the removal of the pesticide imidacloprid [131]. They observed a  
731 maximum adsorption capacity of 8.64 mg/g for imidacloprid on GO/CoFe<sub>2</sub>O<sub>4</sub>-S biochar, which  
732 they attributed to the increased surface area, the  $\pi$ - $\pi$  conjugation interactions between the graphitic  
733 structures/-OH groups and the pollutant, and the abundance of available binding sites such as C-  
734 O, Fe-O, and Co-O.

735 ***Hydrophobic Interactions.*** The non-polar domains of biochar can sequester non-polar  
736 organic compounds, removing them from the aqueous phase. For example, the use of engineered  
737 biochar for the elimination of antibiotics has been well-documented. Zeng et al. activated coffee  
738 ground-derived biochar with H<sub>3</sub>PO<sub>4</sub> to target the adsorption of sulfadiazine [132]. The biochar's  
739 modification led to a significant uptake capacity for sulfadiazine, reaching 139.2 mg/g, which was  
740 primarily due to the hydrophobic effect and  $\pi$ - $\pi$  electron donor-acceptor (EDA) interactions.

741 Additionally, hydrogen bonding, electrostatic forces, and hydrophobic interactions are the  
742 prevalent processes for the removal of organic pollutants in natural environment. For instance, a  
743 sulfur-doped biochar derived from tapioca peel waste proved to be an effective adsorbent for  
744 malachite green (30.2 mg/g) and rhodamine B (33.1 mg/g), with electrostatic attraction, surface  
745 complexation, and hydrogen bonding identified as the primary mechanisms for their removal  
746 [133].

## 747 **5. Future Directions**

748 The next phase of research should build upon the solid foundation laid by current studies,  
749 pushing the boundaries of innovation towards sustainable and scalable solutions. Below are

750 outlined key areas where focused efforts could yield substantial advancements, further solidifying  
751 the role of nano-modified biochar in environmental remediation.

### 752 **5.1 Advancements in Synthesis Methods**

753 The synthesis of nano-modified biochar is a critical area where innovation can  
754 significantly amplify its utility and efficiency. Future research should prioritize the development  
755 of novel synthesis methods that enhance the intrinsic properties of nano-modified biochar, such as  
756 increased surface area, porosity, and reactivity. These improvements could dramatically elevate  
757 its adsorption capacity and effectiveness in pollutant removal. There is a growing need to refine  
758 current methods to make them more energy-efficient and environmentally benign. The exploration  
759 of low-temperature synthesis processes, or the utilization of renewable energy sources, could  
760 contribute to more sustainable production practices. Another key area is the scalability of synthesis  
761 methods. The transition from lab-scale to industrial-scale production often presents challenges in  
762 maintaining the quality and characteristics of nano-modified biochar. Research into scalable  
763 production techniques that can be consistently reproduced will be crucial for widespread  
764 application. The field could also benefit from the exploration of new synthesis techniques, such as  
765 microwave-assisted pyrolysis or hydrothermal carbonization, which might offer unique  
766 advantages in terms of yield, quality, and environmental impact. Tailoring the properties of nano-  
767 modified biochar to target specific pollutants or environmental conditions is another promising  
768 direction. This might involve manipulating the feedstock or the synthesis conditions to produce  
769 nano-modified biochar with specific characteristics suited to target remediation needs.

### 770 **5.2 Enhancing Environmental Sustainability in Biochar Production**

771 In addressing the environmental concerns associated with the calcination process inherent  
772 in biochar production, recent research underscores the importance of implementing innovative

773 strategies to mitigate emissions and optimize sustainability. Optimization of pyrolysis conditions  
774 has been demonstrated to significantly reduce the emission of greenhouse gases and volatile  
775 organic compounds [134]. The integration of advanced emission control technologies, such as  
776 scrubbers and catalytic converters, further enables the effective capture of pollutants, thereby  
777 minimizing atmospheric emissions [135]. Selecting appropriate biomass feedstocks, particularly  
778 those that are waste-derived, can also play a crucial role in reducing environmental impacts by  
779 diverting waste from landfills and reducing methane emissions [136]. Importantly, life cycle  
780 assessments of biochar systems reveal that, when considering the full production and application  
781 cycle, biochar can offer a net positive environmental impact, particularly in terms of carbon  
782 sequestration and soil health improvement, thereby offsetting the emissions generated during its  
783 production [137]. These strategies collectively underscore the multifaceted approach required to  
784 address the environmental challenges of biochar production, emphasizing the need for a balanced  
785 assessment of both its potential environmental impacts and its substantial benefits in  
786 environmental remediation applications.

### 787 **5.3 Assessing and Managing the Environmental Fate of Pollutants in Nano-modified Biochar** 788 **Applications**

789 It is pivotal to address the bioavailability and environmental fate of pollutants once  
790 immobilized by these advanced materials. While nano-modified biochar demonstrates a high  
791 capacity for adsorbing and immobilizing various pollutants due to its large surface area and  
792 enhanced reactivity, the potential for re-release of these pollutants into the environment is a subject  
793 of ongoing research. Factors such as environmental conditions, the properties of the pollutants,  
794 and the physical and chemical characteristics of nano-modified biochar play crucial roles in this  
795 process. An illustrative example of this is the significant impact that environmental pH levels have

796 on the biogeochemical activities of nano-modified biochar in environmental remediation efforts.  
797 Research by Gaya et al. demonstrates that in acidic (low pH) environments, the functional groups  
798 on nano-modified biochar are prone to protonation, leading to the formation of  $H^+$  ions [138]. This  
799 process initiates a competitive interaction between  $H^+$  ions and cationic pollutants for the cation  
800 adsorption sites available on the nano-modified biochar, thereby reducing its pollutant adsorption  
801 capacity, as further evidenced in the studies by Mahmoud et al. and Park et al [139, 140].  
802 Additionally, it was reported that at high pH levels, the surface of nano-modified biochar, which  
803 carries a negative charge, exhibits a lower affinity for negatively charged or neutral pollutants due  
804 to electrostatic repulsion, further complicating the dynamics of pollutant adsorption. Therefore, it  
805 becomes crucial to monitor pH variations in the environment when employing nano-modified  
806 biochar for the purpose of environmental remediation. Adding to this, when nano-modified biochar  
807 is introduced into the environment, its ability to stabilize a significant number of pollutants can  
808 considerably decrease their transport and bioavailability, thereby mitigating their impact on  
809 ecosystems and human health. Yet, the possibility of immobilized pollutants being released back  
810 into the environment remains an unresolved question. This underscores the challenge of retrieving  
811 used biochar from the environment for remediation purposes. Given the nano-scale size of nano-  
812 modified biochar, recycling it poses an even greater challenge. Consequently, the development of  
813 nano-modified biochar recovery technologies and a deeper understanding of its environmental  
814 risks for post-pollutant adsorption warrant further investigation. In addition to the factors  
815 previously mentioned that influence the environmental fate of pollutants immobilized by nano-  
816 modified biochar, the interactions between nano-modified biochar and plant systems represent a  
817 critical area for future investigation. Plants can play a significant role in the uptake and transport  
818 of biochar nanoparticles, potentially leading to bioaccumulation and trophic transfer in the food

819 chain. Consequently, future studies should assess the extent to which nano-modified biochar is  
820 taken up by root systems, its translocation within plant tissues, and its eventual fate in terms of  
821 bioaccumulation and potential food chain transfer. Such research is vital to fully understand the  
822 ecological risks and to develop strategies to mitigate any negative impacts, ensuring that nano-  
823 modified biochar applications in environmental remediation do not inadvertently pose a threat to  
824 ecosystem health or food safety.

#### 825 **5.4 Material Modification and Functionalization**

826 The versatility of nano-modified biochar can be significantly enhanced through strategic  
827 material modification and functionalization. This area of research holds the key to unlocking the  
828 full potential of nano-modified biochar's in environmental applications, particularly pollutant  
829 removal. Tailoring the surface properties of nano-modified biochar through chemical or physical  
830 modifications can significantly improve its affinity for specific pollutants. Investigating various  
831 functional groups that can be introduced onto the biochar surface could lead to more selective and  
832 efficient adsorption processes. The development of nano-modified biochar-based hybrid materials  
833 is an exciting prospect. By combining nano-modified biochar with other materials such as metal  
834 oxides, graphene, or polymers, the resultant composites could exhibit synergistic properties,  
835 enhancing both capacity and selectivity for pollutant removal. Future research should focus on  
836 customizing nano-modified biochar for specific pollutants, which could involve modifying it to  
837 improve its efficiency in adsorbing and breaking down complex organic compounds or heavy  
838 metals. Improving the stability and reusability of nano-modified biochar is crucial for its practical  
839 application. Studies that investigate how modifications impact the durability and regeneration  
840 capacity of nano-modified biochar can lead to more sustainable and economically viable solutions.

#### 841 **6. Conclusion**

842 In this review, we have comprehensively discussed the modification and functionalization  
843 of nano-modified biochars, delving into various preparation and characterization techniques of  
844 biochar-MNPs. We also shed light on the use of these nano-modified biochars in remediating  
845 natural environments where water and soil are contaminated with both heavy metals and organic  
846 substances. The review also reveals that certain characteristics of nano-modified biochars, such as  
847 enhanced surface area, addition of functional groups, and improved electron transport capacity, are  
848 crucial in boosting its efficiency for multifaceted decontamination purposes. Future studies should  
849 delve deeper into the biogeochemical behavior of nano-modified biochar, exploring how its  
850 interactions with soil and water matrices affect the long-term stability and efficacy of contaminant  
851 immobilization. Additionally, understanding the bioavailability of pollutants in the presence of  
852 nano-modified biochar is crucial for evaluating its environmental safety and effectiveness.  
853 Research in these areas will not only broaden our comprehension of nano-modified biochar's  
854 environmental interactions but also refine its applications for sustainable remediation. As nano-  
855 modified biochar continues to emerge as a versatile tool for environmental challenges, its  
856 integration into broader ecological conservation strategies offers a promising path towards  
857 achieving a cleaner and more sustainable planet.

#### 858 **Data availability**

859 No data was generated or used for the research described in the review article.

#### 860 **CRedit authorship contribution statement**

861 **Neda Arabzadeh Nosratabad:** Writing- Original draft preparation and editing. **Qiangu Yan:**  
862 Conceptualization, Writing- Reviewing and Editing. **Zhiyong Cai:** Conceptualization, Writing-  
863 Reviewing and Editing. **Caixia Wan:** Conceptualization, Supervision, Writing- Reviewing and  
864 Editing.

865 **Declaration of Competing Interest**

866 The authors declare that they have no competing interests.

867 **ACKNOWLEDGEMENTS**868 The authors thank the financial support from the USDA Forest Service (Grant No. 23-JV-  
869 11111124-053 and 24-JV-11111124-017).870 **References**

- 871 1. Ramlan, et al., *Pollution and contamination level of Cu, Cd, and Hg heavy metals in soil and food*  
872 *crop*. Int. J. Environ. Sci. Technol., 2022, **19**, 1153-1164. [https://doi.org/10.1007/s13762-021-](https://doi.org/10.1007/s13762-021-03345-8)  
873 [03345-8](https://doi.org/10.1007/s13762-021-03345-8)
- 874 2. Kumar, A., et al., *Lead toxicity: health hazards, influence on food chain, and sustainable*  
875 *remediation approaches*. Int. J. Environ. Res. Public Health., 2020, **17**, 2179.  
876 <https://doi.org/10.3390/ijerph17072179>
- 877 3. Antoniadis, V., et al., *A critical prospective analysis of the potential toxicity of trace element*  
878 *regulation limits in soils worldwide: Are they protective concerning health risk assessment?-A*  
879 *review*. Environ. Int., 2019, **127**, 819-847. <https://doi.org/10.1016/j.envint.2019.03.039>
- 880 4. Shaheen, S.M., et al., *Manganese oxide-modified biochar: production, characterization and*  
881 *applications for the removal of pollutants from aqueous environments-a review*. Bioresour.  
882 Technol., 2022, **346**, 126581. <https://doi.org/10.1016/j.biortech.2021.126581>
- 883 5. Dönmez, G. and N. Koçberber, *Isolation of hexavalent chromium resistant bacteria from industrial*  
884 *saline effluents and their ability of bioaccumulation*. Enzyme Microb. Technol., 2005, **36**, 700-705.  
885 <https://doi.org/10.1016/j.enzmictec.2004.12.025>
- 886 6. Abadeer, N.S., et al., *Distance and plasmon wavelength dependent fluorescence of molecules*  
887 *bound to silica-coated gold nanorods*. ACS nano, 2014, **8**, 8392-8406.  
888 <https://doi.org/10.1021/nn502887j>
- 889 7. Liu, W., et al., *Treatment of CrVI - containing Mg (OH) 2 nanowaste*. Angew. Chem., 2008, **120**,  
890 5701-5704. <https://doi.org/10.1002/ange.200800172>
- 891 8. Kacholi, D.S. and M. Sahu, *Levels and health risk assessment of heavy metals in soil, water, and*  
892 *vegetables of Dar es Salaam, Tanzania*. J. Chem., 2018, **2018**, 1-9.  
893 <https://doi.org/10.1155/2018/1402674>
- 894 9. Kumar, A., et al., *Biochar as environmental armour and its diverse role towards protecting soil,*  
895 *water and air*. Sci. Total Environ., 2022, **806**, 150444.  
896 <https://doi.org/10.1016/j.scitotenv.2021.150444>
- 897 10. Schwartz, J., *Short term fluctuations in air pollution and hospital admissions of the elderly for*  
898 *respiratory disease*. Thorax, 1995, **50**, 531-538. <https://doi.org/10.1136/thx.50.5.531>
- 899 11. Seinfeld, J.H. and S.N. Pandis, *Atmospheric chemistry and physics: from air pollution to climate*  
900 *change*. 2016: John Wiley & Sons.
- 901 12. Bhat, S.A., et al., *Sustainable nanotechnology based wastewater treatment strategies:*  
902 *Achievements, challenges and future perspectives*. Chemosphere, 2022, **288**, 132606.  
903 <https://doi.org/10.1016/j.chemosphere.2021.132606>

- 904 13. Yu, Z., et al., *Physiological and biochemical effects of polystyrene micro/nano plastics on*  
905 *Arabidopsis thaliana*. J. Hazard. Mater., 2024, **469**, 133861.  
906 <https://doi.org/10.1016/j.jhazmat.2024.133861>
- 907 14. Lehmann, J., *A handful of carbon*. Nature, 2007, **447**, 143-144. <https://doi.org/10.1038/447143a>
- 908 15. Liu, Z., et al., *Modified biochar: synthesis and mechanism for removal of environmental heavy*  
909 *metals*. Carbon Research, 2022, **1**, 8. <https://doi.org/10.1007/s44246-022-00007-3>
- 910 16. Amusat, S.O., et al., *Ball-milling synthesis of biochar and biochar-based nanocomposites and*  
911 *prospects for removal of emerging contaminants: A review*. J. Water. Process. Eng., 2021, **41**,  
912 101993. <https://doi.org/10.1016/j.jwpe.2021.101993>
- 913 17. Wardle, D.A., M.-C. Nilsson, and O. Zackrisson, *Fire-derived charcoal causes loss of forest humus*.  
914 Science, 2008, **320**, 629-629. <https://doi.org/10.1126/science.1154960>
- 915 18. Marcińczyk, M. and P. Oleszczuk, *Biochar and engineered biochar as slow-and controlled-release*  
916 *fertilizers*. J. Clean. Prod., 2022, **339**, 130685. <https://doi.org/10.1016/j.jclepro.2022.130685>
- 917 19. Zhang, Y., J. Wang, and Y. Feng, *The effects of biochar addition on soil physicochemical properties:*  
918 *A review*. Catena, 2021, **202**, 105284. <https://doi.org/10.1016/j.catena.2021.105284>
- 919 20. Jia, Q., et al., *Zea mays cultivation, biochar, and arbuscular mycorrhizal fungal inoculation*  
920 *influenced lead immobilization*. Microbiol. Spectr., 2024, **12**, e03427-23.  
921 <https://doi.org/10.1128/spectrum.03427-23>
- 922 21. Elkhalfa, S., et al., *Food waste to biochars through pyrolysis: A review*. Resour. Conserv. Recycl.,  
923 2019, **144**, 310-320. <https://doi.org/10.1016/j.resconrec.2019.01.024>
- 924 22. Zhang, Z., et al., *Insights into biochar and hydrochar production and applications: A review*. Energy,  
925 2019, **171**, 581-598. <https://doi.org/10.1016/j.energy.2019.01.035>
- 926 23. Ahmed, M.B., et al., *Progress in the preparation and application of modified biochar for improved*  
927 *contaminant removal from water and wastewater*. Bioresour. Technol., 2016, **214**, 836-851.  
928 <https://doi.org/10.1016/j.biortech.2016.05.057>
- 929 24. Sizmur, T., et al., *Biochar modification to enhance sorption of inorganics from water*. Bioresour.  
930 technol., 2017, **246**, 34-47. <https://doi.org/10.1016/j.biortech.2017.07.082>
- 931 25. Oliveira, F.R., et al., *Environmental application of biochar: Current status and perspectives*.  
932 Bioresour. technol., 2017, **246**, 110-122. <https://doi.org/10.1016/j.biortech.2017.08.122>
- 933 26. Awang, N.A., et al., *A review on preparation, surface enhancement and adsorption mechanism of*  
934 *biochar - supported nano zero - valent iron adsorbent for hazardous heavy metals*. J. Chem.  
935 Technol. Biotechnol., 2023, **98**, 22-44. <https://doi.org/10.1002/jctb.7182>
- 936 27. Chin, J.F., et al., *Recent development of magnetic biochar crosslinked chitosan on heavy metal*  
937 *removal from wastewater—modification, application and mechanism*. Chemosphere, 2022, **291**,  
938 133035. <https://doi.org/10.1016/j.chemosphere.2021.133035>
- 939 28. Grassian, V.H., *When size really matters: size-dependent properties and surface chemistry of metal*  
940 *and metal oxide nanoparticles in gas and liquid phase environments*. J. Phys. Chem. C., 2008, **112**,  
941 18303-18313. <https://doi.org/10.1021/jp806073t>
- 942 29. Emory, S.R., W.E. Haskins, and S. Nie, *Direct observation of size-dependent optical enhancement*  
943 *in single metal nanoparticles*. J. Am. Chem. Soc., 1998, **120**, 8009-8010.  
944 <https://doi.org/10.1021/ja9815677>
- 945 30. Teow, Y.H. and A.W. Mohammad, *New generation nanomaterials for water desalination: A review*.  
946 Desalination, 2019, **451**, 2-17. <https://doi.org/10.1016/j.desal.2017.11.041>
- 947 31. Rodriguez-Narvaez, O.M., et al., *Biochar-supported nanomaterials for environmental applications*.  
948 J. Ind. Eng.Chem., 2019, **78**, 21-33. <https://doi.org/10.1016/j.jiec.2019.06.008>
- 949 32. Premarathna, K., et al., *Biochar-based engineered composites for sorptive decontamination of*  
950 *water: A review*. Chem. Eng. J., 2019, **372**, 536-550. <https://doi.org/10.1016/j.cej.2019.04.097>

- 951 33. Thines, K., et al., *Synthesis of magnetic biochar from agricultural waste biomass to enhancing*  
952 *route for waste water and polymer application: a review*. *Renew. Sustain. Energy Rev.*, 2017, **67**,  
953 257-276. <https://doi.org/10.1016/j.rser.2016.09.057>
- 954 34. Sultan, H., et al., *Biochar and nano biochar: Enhancing salt resilience in plants and soil while*  
955 *mitigating greenhouse gas emissions: A comprehensive review*. *Environ. Manage.*, 2024, **355**,  
956 120448. <https://doi.org/10.1016/j.jenvman.2024.120448>
- 957 35. Li, R., et al., *An overview of carbothermal synthesis of metal–biochar composites for the removal*  
958 *of oxyanion contaminants from aqueous solution*. *Carbon*, 2018, **129**, 674-687.  
959 <https://doi.org/10.1016/j.carbon.2017.12.070>
- 960 36. Tan, X.-f., et al., *Biochar-based nano-composites for the decontamination of wastewater: a review*.  
961 *Bioresour. Technol.*, 2016, **212**, 318-333. <https://doi.org/10.1016/j.biortech.2016.04.093>
- 962 37. Ahuja, R., et al., *Nano Modifications of Biochar to Enhance Heavy Metal Adsorption from*  
963 *Wastewaters: A Review*. *ACS omega*, 2022, **7**, 45825-45836.  
964 <https://doi.org/10.1021/acsomega.2c05117>
- 965 38. Mašek, O., et al., *Influence of production conditions on the yield and environmental stability of*  
966 *biochar*. *Fuel*, 2013, **103**, 151-155. <https://doi.org/10.1016/j.fuel.2011.08.044>
- 967 39. Demirbas, A., *Effects of temperature and particle size on bio-char yield from pyrolysis of*  
968 *agricultural residues*. *J.Anal. Appl. Pyrolysis*, 2004, **72**, 243-248.  
969 <https://doi.org/10.1016/j.jaap.2004.07.003>
- 970 40. Jiang, M., et al., *Nanobiochar for the remediation of contaminated soil and water: challenges and*  
971 *opportunities*. *Biochar*, 2023, **5**, 2. <https://doi.org/10.1007/s42773-022-00201-x>
- 972 41. Alsawy, T., et al., *A comprehensive review on the chemical regeneration of biochar adsorbent for*  
973 *sustainable wastewater treatment*. *Npj Clean Water*, 2022, **5**, 29. [https://doi.org/10.1038/s41545-](https://doi.org/10.1038/s41545-022-00172-3)  
974 [022-00172-3](https://doi.org/10.1038/s41545-022-00172-3)
- 975 42. Singh, P., et al., *Sustainable low-concentration arsenite [As (III)] removal in single and*  
976 *multicomponent systems using hybrid iron oxide–biochar nanocomposite adsorbents—A*  
977 *mechanistic study*. *ACS Omega*, 2020, **5**, 2575-2593. <https://doi.org/10.1021/acsomega.9b02842>
- 978 43. Zhang, M. and B. Gao, *Removal of arsenic, methylene blue, and phosphate by biochar/AlOOH*  
979 *nanocomposite*. *Chem. Engin. J.*, 2013, **226**, 286-292. <https://doi.org/10.1016/j.cej.2013.04.077>
- 980 44. Jung, K.-W. and K.-H. Ahn, *Fabrication of porosity-enhanced MgO/biochar for removal of*  
981 *phosphate from aqueous solution: application of a novel combined electrochemical modification*  
982 *method*. *Bioresour. Technol.*, 2016, **200**, 1029-1032.  
983 <https://doi.org/10.1016/j.biortech.2015.10.008>
- 984 45. Li, A.Y., et al., *Superefficient removal of heavy metals from wastewater by Mg-loaded biochars:*  
985 *Adsorption characteristics and removal mechanisms*. *Langmuir*, 2020, **36**, 9160-9174.  
986 <https://doi.org/10.1021/acs.langmuir.0c01454>
- 987 46. Li, C., et al., *Facile synthesis of nano ZnO/ZnS modified biochar by directly pyrolyzing of zinc*  
988 *contaminated corn stover for Pb (II), Cu (II) and Cr (VI) removals*. *Waste Management*, 2018, **79**,  
989 625-637. <https://doi.org/10.1016/j.wasman.2018.08.035>
- 990 47. Chaukura, N., E.C. Murimba, and W. Gwenzi, *Synthesis, characterisation and methyl orange*  
991 *adsorption capacity of ferric oxide–biochar nano-composites derived from pulp and paper sludge*.  
992 *Appl. Water Sci.*, 2017, **7**, 2175-2186. <https://doi.org/10.1007/s13201-016-0392-5>
- 993 48. Yang, F., et al., *A novel electrochemical modification combined with one-step pyrolysis for*  
994 *preparation of sustainable thorn-like iron-based biochar composites*. *Bioresour. Technol.*, 2019,  
995 **274**, 379-385. <https://doi.org/10.1016/j.biortech.2018.10.042>
- 996 49. Zhu, N., et al., *Adsorption of arsenic, phosphorus and chromium by bismuth impregnated biochar:*  
997 *Adsorption mechanism and depleted adsorbent utilization*. *Chemosphere*, 2016, **164**, 32-40.  
998 <https://doi.org/10.1016/j.chemosphere.2016.08.036>

- 999 50. Omidvar-Hosseini, F. and F. Moeinpour, *Removal of Pb (II) from aqueous solutions using Acacia*  
1000 *Nilotica seed shell ash supported NiO. 5ZnO. 5Fe2O4 magnetic nanoparticles*. J. Water Reuse  
1001 Desalin., 2016, **6**, 562-573. <https://doi.org/10.2166/wrd.2016.073>
- 1002 51. Chen, Q., et al., *Synthesis of a stable magnesium-impregnated biochar and its reduction of*  
1003 *phosphorus leaching from soil*. Chemosphere, 2018, **199**, 402-408.  
1004 <https://doi.org/10.1016/j.chemosphere.2018.02.058>
- 1005 52. Gupta, V. and A. Nayak, *Cadmium removal and recovery from aqueous solutions by novel*  
1006 *adsorbents prepared from orange peel and Fe2O3 nanoparticles*. Chem. Engin J., 2012, **180**, 81-  
1007 90. <https://doi.org/10.1016/j.cej.2011.11.006>
- 1008 53. Dai, L., et al., *Calcium-rich biochar from the pyrolysis of crab shell for phosphorus removal*. J.  
1009 Environ. Manage., 2017, **198**, 70-74. <https://doi.org/10.1016/j.jenvman.2017.04.057>
- 1010 54. Inyang, M., et al., *Synthesis, characterization, and dye sorption ability of carbon nanotube–biochar*  
1011 *nanocomposites*. Chem. Engin. J., 2014, **236**, 39-46. <https://doi.org/10.1016/j.cej.2013.09.074>
- 1012 55. Jabasingh, S.A., H. Belachew, and A. Yimam, *Iron oxide induced bagasse nanoparticles for the*  
1013 *sequestration of Cr6+ ions from tannery effluent using a modified batch reactor*. J. Appl. Polym.  
1014 Sci., 2018, **135**, 46683. <https://doi.org/10.1002/app.46683>
- 1015 56. Zhang, H., et al., *Enhanced removal of heavy metal ions from aqueous solution using manganese*  
1016 *dioxide-loaded biochar: Behavior and mechanism*. Sci. Rep., 2020, **10**, 6067.  
1017 <https://doi.org/10.1038/s41598-020-63000-z>
- 1018 57. Zhou, L., et al., *Adsorption properties of nano-MnO2–biochar composites for copper in aqueous*  
1019 *solution*. Molecules, 2017, **22**, 173. <https://doi.org/10.3390/molecules22010173>
- 1020 58. Diao, Z.-H., et al., *Insights into the simultaneous removal of Cr6+ and Pb2+ by a novel sewage*  
1021 *sludge-derived biochar immobilized nanoscale zero valent iron: Coexistence effect and mechanism*.  
1022 Sci. Total Environ., 2018, **642**, 505-515. <https://doi.org/10.1016/j.scitotenv.2018.06.093>
- 1023 59. Kim, J., et al., *Application of iron-modified biochar for arsenite removal and toxicity reduction*. J.  
1024 Ind. Eng. Chem., 2019, **80**, 17-22. <https://doi.org/10.1016/j.jiec.2019.07.026>
- 1025 60. Wan, S., et al., *Functionalizing biochar with Mg–Al and Mg–Fe layered double hydroxides for*  
1026 *removal of phosphate from aqueous solutions*. J. Ind. Eng. Chem., 2017, **47**, 246-253.  
1027 <https://doi.org/10.1016/j.jiec.2016.11.039>
- 1028 61. Tomczyk, A. and K. Szweczek-Karpisz, *Effect of biochar modification by vitamin c, hydrogen*  
1029 *peroxide or silver nanoparticles on its physicochemistry and tetracycline removal*. Materials, 2022,  
1030 **15**, 5379. <https://doi.org/10.3390/ma15155379>
- 1031 62. Zhang, X. and R. Sun, *Construction of an electrochemical sensor for detection of nitrite by gold*  
1032 *nanoparticles immobilized on biochar*. Int. J. Electrochem. Sci., 2023, 100219.  
1033 <https://doi.org/10.1016/j.ijoes.2023.100219>
- 1034 63. Wang, J., et al., *Gold nanoparticles decorated biochar modified electrode for the high-performance*  
1035 *simultaneous determination of hydroquinone and catechol*. Sens. Actuators B: Chem., 2020, **306**,  
1036 127590. <https://doi.org/10.1016/j.snb.2019.127590>
- 1037 64. Zhu, S., et al., *Magnetic nanoscale zerovalent iron assisted biochar: interfacial chemical behaviors*  
1038 *and heavy metals remediation performance*. ACS Sustain. Chem. Eng., 2017, **5**, 9673-9682.  
1039 <https://doi.org/10.1021/acssuschemeng.7b00542>
- 1040 65. Liao, T., et al., *La (OH) 3-modified magnetic pineapple biochar as novel adsorbents for efficient*  
1041 *phosphate removal*. Bioresour. Technol., 2018, **263**, 207-213.  
1042 <https://doi.org/10.1016/j.biortech.2018.04.108>
- 1043 66. Arabyarmohammadi, H., et al., *Utilization of a novel chitosan/clay/biochar nanobiocomposite for*  
1044 *immobilization of heavy metals in acid soil environment*. J. Polym. Environ., 2018, **26**, 2107-2119.  
1045 <https://doi.org/10.1007/s10924-017-1102-6>

- 1046 67. Daraei, P., et al., *Novel thin film composite membrane fabricated by mixed matrix*  
1047 *nanoclay/chitosan on PVDF microfiltration support: Preparation, characterization and*  
1048 *performance in dye removal.* J. Membr. Sci., 2013, **436**, 97-108.  
1049 <https://doi.org/10.1016/j.memsci.2013.02.031>
- 1050 68. Krajewska, B., *Diffusion of metal ions through gel chitosan membranes.* React. Funct. Polym., 2001,  
1051 **47**, 37-47. [https://doi.org/10.1016/S1381-5148\(00\)00068-7](https://doi.org/10.1016/S1381-5148(00)00068-7)
- 1052 69. Liu, G., et al., *Formation and Physicochemical Characteristics of Nano Biochar: Insight into*  
1053 *Chemical and Colloidal Stability.* Environ. Sci. Technol., 2018, **52**, 10369-10379.  
1054 <https://doi.org/10.1021/acs.est.8b01481>
- 1055 70. Wang, D., W. Zhang, and D. Zhou, *Antagonistic Effects of Humic Acid and Iron Oxyhydroxide Grain-*  
1056 *Coating on Biochar Nanoparticle Transport in Saturated Sand.* Environ. Sci. Technol., 2013, **47**,  
1057 5154-5161. <https://doi.org/10.1021/es305337r>
- 1058 71. Kumar, M., et al., *Ball milling as a mechanochemical technology for fabrication of novel biochar*  
1059 *nanomaterials.* Bioresour. Technol., 2020, **312**, 123613.  
1060 <https://doi.org/10.1016/j.biortech.2020.123613>
- 1061 72. Song, B., et al., *Preparation of nano-biochar from conventional biorefineries for high-value*  
1062 *applications.* Renew. Sustain. Energy Rev., 2022, **157**, 112057.  
1063 <https://doi.org/10.1016/j.rser.2021.112057>
- 1064 73. Lyu, H., et al., *Effects of ball milling on the physicochemical and sorptive properties of biochar:*  
1065 *Experimental observations and governing mechanisms.* Environ. Pollut., 2018, **233**, 54-63.  
1066 <https://doi.org/10.1016/j.envpol.2017.10.037>
- 1067 74. Kumar, A., et al., *Sustainable nano-hybrids of magnetic biochar supported g-C<sub>3</sub>N<sub>4</sub>/FeVO<sub>4</sub> for solar*  
1068 *powered degradation of noxious pollutants- Synergism of adsorption, photocatalysis & photo-*  
1069 *ozonation.* J. Clean. Prod., 2017, **165**, 431-451. <https://doi.org/10.1016/j.jclepro.2017.07.117>
- 1070 75. Wu, H., et al., *Modified biochar supported Ag/Fe nanoparticles used for removal of cephalixin in*  
1071 *solution: Characterization, kinetics and mechanisms.* Colloids Surf. A: Physicochem. Eng., 2017,  
1072 **517**, 63-71. <https://doi.org/10.1016/j.colsurfa.2017.01.005>
- 1073 76. Lian, F. and B. Xing, *Black Carbon (Biochar) In Water/Soil Environments: Molecular Structure,*  
1074 *Sorption, Stability, and Potential Risk.* Environ. Sci. Technol., 2017, **51**, 13517-13532.  
1075 <https://doi.org/10.1021/acs.est.7b02528>
- 1076 77. Liu, Z., et al., *Biochar particle size, shape, and porosity act together to influence soil water*  
1077 *properties.* Plos one, 2017, **12**, e0179079. <https://doi.org/10.1371/journal.pone.0179079>
- 1078 78. Pignatello, J.J., W.A. Mitch, and W. Xu, *Activity and Reactivity of Pyrogenic Carbonaceous Matter*  
1079 *toward Organic Compounds.* Environ. Sci. Technol., 2017, **51**, 8893-8908.  
1080 <https://doi.org/10.1021/acs.est.7b01088>
- 1081 79. Yang, F., et al., *Porous biochar composite assembled with ternary needle-like iron-manganese-*  
1082 *sulphur hybrids for high-efficiency lead removal.* Bioresour. Technol., 2019, **272**, 415-420.  
1083 <https://doi.org/10.1016/j.biortech.2018.10.068>
- 1084 80. Xiang, Y., et al., *Biochar decorated with gold nanoparticles for electrochemical sensing application.*  
1085 *Electrochim. Acta.*, 2018, **261**, 464-473. <https://doi.org/10.1016/j.electacta.2017.12.162>
- 1086 81. Wang, C. and H. Wang, *Pb(II) sorption from aqueous solution by novel biochar loaded with nano-*  
1087 *particles.* Chemosphere, 2018, **192**, 1-4. <https://doi.org/10.1016/j.chemosphere.2017.10.125>
- 1088 82. Yang, B., et al., *Lanthanum ferrite nanoparticles modification onto biochar: derivation from four*  
1089 *different methods and high performance for phosphate adsorption.* Environ. Sci. Pollut. Res., 2019,  
1090 **26**, 22010-22020. <https://doi.org/10.1007/s11356-019-04553-z>
- 1091 83. Zhang, M., et al., *Synthesis of porous MgO-biochar nanocomposites for removal of phosphate and*  
1092 *nitrate from aqueous solutions.* Chem. Eng. J., 2012, **210**, 26-32.  
1093 <https://doi.org/10.1016/j.cej.2012.08.052>

- 1094 84. Li, R., et al., *Recovery of phosphate from aqueous solution by magnesium oxide decorated*  
1095 *magnetic biochar and its potential as phosphate-based fertilizer substitute*. *Bioresour. Technol.*,  
1096 2016, **215**, 209-214. <https://doi.org/10.1016/j.biortech.2016.02.125>
- 1097 85. Liu, N., et al., *Removal mechanisms of aqueous Cr(VI) using apple wood biochar: a spectroscopic*  
1098 *study*. *J. Hazard. Mater.*, 2020, **384**, 121371. <https://doi.org/10.1016/j.jhazmat.2019.121371>
- 1099 86. Feng, Y., et al., *Distribution and speciation of iron in Fe-modified biochars and its application in*  
1100 *removal of As(V), As(III), Cr(VI), and Hg(II): An X-ray absorption study*. *J. Hazard. Mater.*, 2020, **384**,  
1101 121342. <https://doi.org/10.1016/j.jhazmat.2019.121342>
- 1102 87. Goswami, L., et al., *Nano-biochar as a sustainable catalyst for anaerobic digestion: a synergetic*  
1103 *closed-loop approach*. *Catalysts*, 2022, **12**, 186. <https://doi.org/10.3390/catal12020186>
- 1104 88. Jiang, C., et al., *Converting waste lignin into nano-biochar as a renewable substitute of carbon*  
1105 *black for reinforcing styrene-butadiene rubber*. *Waste Manage.*, 2020, **102**, 732-742.  
1106 <https://doi.org/10.1016/j.wasman.2019.11.019>
- 1107 89. Xia, C., et al., *Remediation competence of nanoparticles amalgamated biochar*  
1108 *(nanobiochar/nanocomposite) on pollutants: A review*. *Environ. Res.*, 2023, **218**, 114947.  
1109 <https://doi.org/10.1016/j.envres.2022.114947>
- 1110 90. Yang, J., et al., *Degradation of p-nitrophenol by lignin and cellulose chars: H2O2-mediated reaction*  
1111 *and direct reaction with the char*. *Environ. Sci. Technol.*, 2017, **51**, 8972-8980.  
1112 <https://doi.org/10.1021/acs.est.7b01087>
- 1113 91. He, R., et al., *Activated biochar with iron-loading and its application in removing Cr (VI) from*  
1114 *aqueous solution*. *Colloids Surf. A Physicochem. Eng. Asp.*, 2019, **579**, 123642.  
1115 <https://doi.org/10.1016/j.colsurfa.2019.123642>
- 1116 92. Zheng, J., et al., *Levels, Spatial Distribution, and Impact Factors of Heavy Metals in the Hair of*  
1117 *Metropolitan Residents in China and Human Health Implications*. *Environ. Sci. Technol.*, 2021, **55**,  
1118 10578-10588. <https://doi.org/10.1021/acs.est.1c02001>
- 1119 93. Wan, X., C. Li, and S.J. Parikh, *Simultaneous removal of arsenic, cadmium, and lead from soil by*  
1120 *iron-modified magnetic biochar*. *Environ. Pollut.*, 2020, **261**, 114157.  
1121 <https://doi.org/10.1016/j.envpol.2020.114157>
- 1122 94. Zhu, L., et al., *Coupling interaction between porous biochar and nano zero valent iron/nano  $\alpha$ -*  
1123 *hydroxyl iron oxide improves the remediation efficiency of cadmium in aqueous solution*.  
1124 *Chemosphere*, 2019, **219**, 493-503. <https://doi.org/10.1016/j.chemosphere.2018.12.013>
- 1125 95. Zhang, G., et al., *Effect of Fe–Mn–Ce modified biochar composite on microbial diversity and*  
1126 *properties of arsenic-contaminated paddy soils*. *Chemosphere*, 2020, **250**, 126249.  
1127 <https://doi.org/10.1016/j.chemosphere.2020.126249>
- 1128 96. Rafique, M.I., et al., *Immobilization and mitigation of chromium toxicity in aqueous solutions and*  
1129 *tannery waste-contaminated soil using biochar and polymer-modified biochar*. *Chemosphere*,  
1130 2021, **266**, 129198. <https://doi.org/10.1016/j.chemosphere.2020.129198>
- 1131 97. Shakya, A., M. Vithanage, and T. Agarwal, *Influence of pyrolysis temperature on biochar properties*  
1132 *and Cr(VI) adsorption from water with groundnut shell biochars: Mechanistic approach*. *Environ.*  
1133 *Res.*, 2022, **215**, 114243. <https://doi.org/10.1016/j.envres.2022.114243>
- 1134 98. Wafiq, A., D. Reichel, and M. Hanafy, *Pressure influence on pyrolysis product properties of raw and*  
1135 *torrefied Miscanthus: Role of particle structure*. *Fuel*, 2016, **179**, 156-167.  
1136 <https://doi.org/10.1016/j.fuel.2016.03.092>
- 1137 99. Lian, L., et al., *Globalization-Driven Industry Relocation Significantly Reduces Arctic PAH*  
1138 *Contamination*. *Environ. Sci. Technol.*, 2022, **56**, 145-154.  
1139 <https://doi.org/10.1021/acs.est.1c05198>

- 1140 100. Tian, H., et al., *Degradation Prediction and Products of Polycyclic Aromatic Hydrocarbons in Soils*  
1141 *by Highly Active Bimetals/AC-Activated Persulfate*. ACS ES&T Eng., 2021, **1**, 1183-1192.  
1142 <https://doi.org/10.1021/acsestengg.1c00063>
- 1143 101. Li, H., F. Zhu, and S. He, *The degradation of decabromodiphenyl ether in the e-waste site by biochar*  
1144 *supported nanoscale zero-valent iron /persulfate*. Ecotoxicol. Environ. Saf., 2019, **183**, 109540.  
1145 <https://doi.org/10.1016/j.ecoenv.2019.109540>
- 1146 102. Wei, X., et al., *Facile Ball-Milling Synthesis of CuO/Biochar Nanocomposites for Efficient Removal*  
1147 *of Reactive Red 120*. ACS Omega, 2020, **5**, 5748-5755.  
1148 <https://doi.org/10.1021/acsomega.9b03787>
- 1149 103. Ma, S., et al., *New insights into contrasting mechanisms for PAE adsorption on millimeter, micron-*  
1150 *and nano-scale biochar*. Environ. Sci. Pollut. Res., 2019, **26**, 18636-18650.  
1151 <https://doi.org/10.1007/s11356-019-05181-3>
- 1152 104. Xu, Y., et al., *Effects of Fe-Mn oxide-modified biochar composite applications on phthalate esters*  
1153 *(PAEs) accumulation in wheat grains and grain quality under PAEs-polluted brown soil*. Ecotoxicol.  
1154 Environ. Saf., 2021, **208**, 111624. <https://doi.org/10.1016/j.ecoenv.2020.111624>
- 1155 105. Bentley, M.J., et al., *Pre-pyrolysis metal and base addition catalyzes pore development and*  
1156 *improves organic micropollutant adsorption to pine biochar*. Chemosphere, 2022, **286**, 131949.  
1157 <https://doi.org/10.1016/j.chemosphere.2021.131949>
- 1158 106. Zhang, Y., et al., *Bacterial response to soil property changes caused by wood ash from wildfire in*  
1159 *forest soils around mining areas: Relevance of bacterial community composition, carbon and*  
1160 *nitrogen cycling*. J. Hazard. Mater., 2021, **412**, 125264.  
1161 <https://doi.org/10.1016/j.jhazmat.2021.125264>
- 1162 107. Fu, H., et al., *Photochemistry of Dissolved Black Carbon Released from Biochar: Reactive Oxygen*  
1163 *Species Generation and Phototransformation*. Environ. Sci. Technol., 2016, **50**, 1218-1226.  
1164 <https://doi.org/10.1021/acs.est.5b04314>
- 1165 108. Ibrahim, M.M., et al., *Field-applied biochar-based MgO and sepiolite composites possess CO<sub>2</sub>*  
1166 *capture potential and alter organic C mineralization and C-cycling bacterial structure in fertilized*  
1167 *soils*. Sci. Total Environ., 2022, **813**, 152495. <https://doi.org/10.1016/j.scitotenv.2021.152495>
- 1168 109. Zheng, T., S. Ouyang, and Q. Zhou, *Synthesis, characterization, safety design, and application of*  
1169 *NPs@ BC for contaminated soil remediation and sustainable agriculture*. Biochar, 2023, **5**, 5.  
1170 <https://doi.org/10.1007/s42773-022-00198-3>
- 1171 110. Creamer, A.E., B. Gao, and M. Zhang, *Carbon dioxide capture using biochar produced from*  
1172 *sugarcane bagasse and hickory wood*. Chem. Eng. J., 2014, **249**, 174-179.  
1173 <https://doi.org/10.1016/j.cej.2014.03.105>
- 1174 111. Creamer, A.E., B. Gao, and S. Wang, *Carbon dioxide capture using various metal oxyhydroxide-*  
1175 *biochar composites*. Chem. Eng. J., 2016, **283**, 826-832. <https://doi.org/10.1016/j.cej.2015.08.037>
- 1176 112. Kumar, A., et al., *Sorption of volatile organic compounds on non-activated biochar*. Bioresour.  
1177 Technol., 2020, **297**, 122469. <https://doi.org/10.1016/j.biortech.2019.122469>
- 1178 113. Cheng, N., et al., *Adsorption of emerging contaminants from water and wastewater by modified*  
1179 *biochar: A review*. Environ. Pollut., 2021, **273**, 116448.  
1180 <https://doi.org/10.1016/j.envpol.2021.116448>
- 1181 114. Ambaye, T., et al., *Mechanisms and adsorption capacities of biochar for the removal of organic*  
1182 *and inorganic pollutants from industrial wastewater*. Int. J. Environ. Sci. Technol., 2021, 1-22.  
1183 <https://doi.org/10.1007/s13762-020-03060-w>
- 1184 115. Zhang, H., et al., *Enhanced aqueous Cr (VI) removal using chitosan-modified magnetic biochars*  
1185 *derived from bamboo residues*. Chemosphere, 2020, **261**, 127694.  
1186 <https://doi.org/10.1016/j.chemosphere.2020.127694>

- 1187 116. Chen, H., et al., *KOH modification effectively enhances the Cd and Pb adsorption performance of*  
 1188 *N-enriched biochar derived from waste chicken feathers*. Waste Manag., 2021, **130**, 82-92.  
 1189 <https://doi.org/10.1016/j.wasman.2021.05.015>
- 1190 117. Chen, M., et al., *Facilitated transport of cadmium by biochar-Fe<sub>3</sub>O<sub>4</sub> nanocomposites in water-*  
 1191 *saturated natural soils*. Sci. Total. Environ., 2019, **684**, 265-275.  
 1192 <https://doi.org/10.1016/j.scitotenv.2019.05.326>
- 1193 118. Zhang, S., et al., *A novel biochar supported CMC stabilized nano zero-valent iron composite for*  
 1194 *hexavalent chromium removal from water*. Chemosphere, 2019, **217**, 686-694.  
 1195 <https://doi.org/10.1016/j.chemosphere.2018.11.040>
- 1196 119. Jia, X., et al., *The antimony sorption and transport mechanisms in removal experiment by Mn-*  
 1197 *coated biochar*. Sci. Total Environ., 2020, **724**, 138158.  
 1198 <https://doi.org/10.1016/j.scitotenv.2020.138158>
- 1199 120. Chen, H., et al., *Enhanced sorption of trivalent antimony by chitosan-loaded biochar in aqueous*  
 1200 *solutions: characterization, performance and mechanisms*. J. Hazard. Mater., 2022, **425**, 127971.  
 1201 <https://doi.org/10.1016/j.jhazmat.2021.127971>
- 1202 121. Wang, L., et al., *Enhanced antimonate (Sb (V)) removal from aqueous solution by La-doped*  
 1203 *magnetic biochars*. Chem. Eng. J., 2018, **354**, 623-632. <https://doi.org/10.1016/j.cej.2018.08.074>
- 1204 122. Murtaza, G., et al., *Biochar as a green sorbent for remediation of polluted soils and associated*  
 1205 *toxicity risks: A critical review*. Separations, 2023, **10**, 197.  
 1206 <https://doi.org/10.3390/separations10030197>
- 1207 123. Yu, C., et al., *Removal of Cu (ii) from aqueous solution using Fe<sub>3</sub>O<sub>4</sub>-alginate modified biochar*  
 1208 *microspheres*. RSC Adv., 2017, **7**, 53135-53144. <https://doi.org/10.1039/C7RA10185F>
- 1209 124. Yuan, Y., et al., *Applications of biochar in redox-mediated reactions*. Bioresour. Technol., 2017, **246**,  
 1210 271-281. <https://doi.org/10.1016/j.biortech.2017.06.154>
- 1211 125. Wen, E., et al., *Iron-modified biochar and water management regime-induced changes in plant*  
 1212 *growth, enzyme activities, and phytoavailability of arsenic, cadmium and lead in a paddy soil*. J.  
 1213 Hazard. Mater., 2021, **407**, 124344. <https://doi.org/10.1016/j.jhazmat.2020.124344>
- 1214 126. Liang, H., et al., *Preparation of nitrogen-doped porous carbon material by a hydrothermal-*  
 1215 *activation two-step method and its high-efficiency adsorption of Cr (VI)*. J. Hazard. Mater., 2020,  
 1216 **387**, 121987. <https://doi.org/10.1016/j.jhazmat.2019.121987>
- 1217 127. Wang, X., et al., *Recent advances in biochar application for water and wastewater treatment: a*  
 1218 *review*. PeerJ, 2020, **8**, e9164. <https://doi.org/10.7717/peerj.9164>
- 1219 128. Chen, Z., B. Chen, and C.T. Chiou, *Fast and slow rates of naphthalene sorption to biochars produced*  
 1220 *at different temperatures*. Environ. Sci. Technol., 2012, **46**, 11104-11111.  
 1221 <https://doi.org/10.1021/es302345e>
- 1222 129. Zhu, X., et al., *A novel porous carbon derived from hydrothermal carbon for efficient adsorption of*  
 1223 *tetracycline*. Carbon, 2014, **77**, 627-636. <https://doi.org/10.1016/j.carbon.2014.05.067>
- 1224 130. Xie, M., et al., *Adsorption of sulfonamides to demineralized pine wood biochars prepared under*  
 1225 *different thermochemical conditions*. Environ. Pollut., 2014, **186**, 187-194.  
 1226 <https://doi.org/10.1016/j.envpol.2013.11.022>
- 1227 131. Ma, Y., et al., *A novel, efficient and sustainable magnetic sludge biochar modified by graphene*  
 1228 *oxide for environmental concentration imidacloprid removal*. J. Hazard. Mater., 2021, **407**, 124777.  
 1229 <https://doi.org/10.1016/j.jhazmat.2020.124777>
- 1230 132. Zeng, X.-Y., et al., *Impacts of temperatures and phosphoric-acid modification to the*  
 1231 *physicochemical properties of biochar for excellent sulfadiazine adsorption*. Biochar, 2022, **4**, 14.  
 1232 <https://doi.org/10.1007/s42773-022-00143-4>

- 1233 133. Vigneshwaran, S., et al., *Fabrication of sulfur-doped biochar derived from tapioca peel waste with superior adsorption performance for the removal of Malachite green and Rhodamine B dyes*. Surf. Interf., 2021, **23**, 100920. <https://doi.org/10.1016/j.surfin.2020.100920>
- 1234
- 1235
- 1236 134. Safarian, S., *Performance analysis of sustainable technologies for biochar production: A comprehensive review*. Energy Rep., 2023, **9**, 4574-4593. <https://doi.org/10.1016/j.egy.2023.03.111>
- 1237
- 1238
- 1239 135. Li, S., *Reviewing Air Pollutants Generated during the Pyrolysis of Solid Waste for Biofuel and Biochar Production: Toward Cleaner Production Practices*. Sustainability, 2024, **16**, 1169. <https://doi.org/10.3390/su16031169>
- 1240
- 1241
- 1242 136. Feng, D., et al., *Review of Carbon Fixation Evaluation and Emission Reduction Effectiveness for Biochar in China*. Energy & Fuels, 2020, **34**, 10583-10606. <https://doi.org/10.1021/acs.energyfuels.0c02396>
- 1243
- 1244
- 1245 137. Roberts, K.G., et al., *Life Cycle Assessment of Biochar Systems: Estimating the Energetic, Economic, and Climate Change Potential*. Environ. Sci. Technol., 2010, **44**, 827-833. <https://doi.org/10.1021/es902266r>
- 1246
- 1247
- 1248 138. Gaya, U.I., E. Otene, and A.H. Abdullah, *Adsorption of aqueous Cd (II) and Pb (II) on activated carbon nanopores prepared by chemical activation of doum palm shell*. SpringerPlus, 2015, **4**, 1-18. <https://doi.org/10.1186/s40064-015-1256-4>
- 1249
- 1250
- 1251 139. Mahmoud, M.E., N.A. Fekry, and A.M. Abdelfattah, *A novel nanobiosorbent of functionalized graphene quantum dots from rice husk with barium hydroxide for microwave enhanced removal of lead (II) and lanthanum (III)*. Bioresour. Technol., 2020, **298**, 122514. <https://doi.org/10.1016/j.biortech.2019.122514>
- 1252
- 1253
- 1254
- 1255 140. Park, J.-H., et al., *Removing mercury from aqueous solution using sulfurized biochar and associated mechanisms*. Environ. Pollut., 2019, **244**, 627-635. <https://doi.org/10.1016/j.envpol.2018.10.069>
- 1256

1257 **Table 1.** Summary of Biomass Modifications for Metal Nanocomposite Synthesis and Applications

Feedstock	Metal/Organic or Inorganic Precursor	Pyrolysis Condition	Formed Nanocomposite	Application	Adsorption Efficiency	Adsorption Capacity	Ref
Corn stalk	FeCl <sub>3</sub> pretreatment in an electric field	600 °C	EC-Fe <sub>3</sub> O <sub>4</sub> -biochar	Adsorption of Pb(II) ions from wastewater	Not mentioned	113 mg/g	[48]
Wheat straw	Bi <sub>2</sub> O <sub>3</sub> and hydrochloric acid	400-600 °C	Bismuth-impregnated biochar	Absorption of P, As(III), and Cr(VI)	Not mentioned	P = 125.40 mg/g As(III) = 16.21 mg/g Cr(VI) = 12.23 mg/g	[49]
Paper and paper sludge (PPS)	FeCl <sub>3</sub>	750 °C	Fe <sub>2</sub> O <sub>3</sub> -biochar	Removal of methyl orange (MO) from contaminated wastewater	52.79% higher than that of pristine biochar	20.53 mg/g	[47]
Acacia Nilotica seed shell ash (ANSA)	Nickel and zinc salts	550 °C	Ni <sub>0.5</sub> Zn <sub>0.5</sub> Fe <sub>2</sub> O <sub>4</sub> on ANSA	Adsorption of Pb(II) ions from water	94.8%, using 0.05 g of adsorbent and 50 mg/L Pb (II)	maximum monolayer adsorption capacity of 37.6 mg/g	[50]
Zinc-contaminated corn stover biomass	Zinc compounds	Slow pyrolysis (different temperatures: 500, 600, 700, and 800 °C)	ZnO/ZnS-modified biochar	Absorption of Pb(II), Cu(II), and Cr(VI)	~ 99%	Pb(II) = 135.8 mg/g Cu(II) = 91.2 mg/g Cr(VI) = 24.5 mg/g	[46]

Cow dung	Magnesium	600 °C	MgO-biochar Composite	Reduce leaching of phosphorus from soil	89.25%	30 mg/g	[51]
Orange peel powder (OPP)	Ferric chloride hexahydrate and ferrous sulfate heptahydrate	Coprecipitation (low-temperature method)	Fe <sub>3</sub> O <sub>4</sub> -OPP (MNP-OPP)	Removal of cadmium ions from aqueous solutions	82%	76.92 mg/g	[52]
Crab shells	Naturally present calcium in crab shells	300 to 900°C	Calcite-based and lime-based CRB	Phosphorus removal or recovery from wastewater	26% to 100% for a phosphate solution 1% to 63% for anaerobic digestion effluent	Not mentioned	[53]
Carboxyl-functionalized CNT-impregnated biochar	Carbon nanotubes (CNT)	Slow pyrolysis (600 °C)	biochar-CNT	Sorption of methylene blue	47%-64%	2.4 mg/g for HC-CNT-1% 5.5 mg/g for biochar-CNT-1%	[54]

1258

1259

1260

1261

1262

1263 **Table 2.** Overview of Modified Biochar Nanocomposites: Feedstock Sources, Metal Precursors, Pyrolysis Techniques, and Remediation  
 1264 Applications

Feedstock	Metal/Organic or Inorganic Precursor	Pyrolysis Condition	Formed Nanocomposite	Application	Adsorption Efficiency	Adsorption Capacity	Ref
Invasive water hyacinth	Manganese Dioxide	Slow pyrolysis at low temperature (450 °C)	MnO <sub>2</sub> -biochar	Adsorption of Cd(II), Cu(II), Zn(II), Pb(II)	Not mentioned	Cd (II) = 232.5 mg/g Cu (II) = 248.9 mg/g Zn (II) = 239.4 mg/g Pb (II) = 249.2 mg/g	[56]
Sewage sludge	Zero-Valent Iron	600 °C for 3 h, 10 °C/min in N <sub>2</sub> atmosphere	SSB-nZVI	Removal of Cr <sup>6+</sup> and Pb <sup>2+</sup> ions	Cr <sup>6+</sup> = 90% Pb <sup>2+</sup> = 82%	Not mentioned	[58]
Miscanthus	Amorphous Iron (hydr)oxide	500 °C for an h, 10 °C/min in a N <sub>2</sub> atmosphere	Fe-modified biochar	Arsenite adsorption	Not mentioned	Arsenite powder = 56.06 mg/g Arsenite beads = 47.90 mg/g	[59]
Bamboo	Mg-Al and Mg-Fe LDHs	600°C for 2 h	Mg-Al/Mg-Fe LDH-modified biochar	Phosphate removal from water	95%	Mg-Fe LDH (40%)/biochar= 7.58 mg/g Mg-Al LDH (40%)/biochar= 13.11 mg/g	[60]

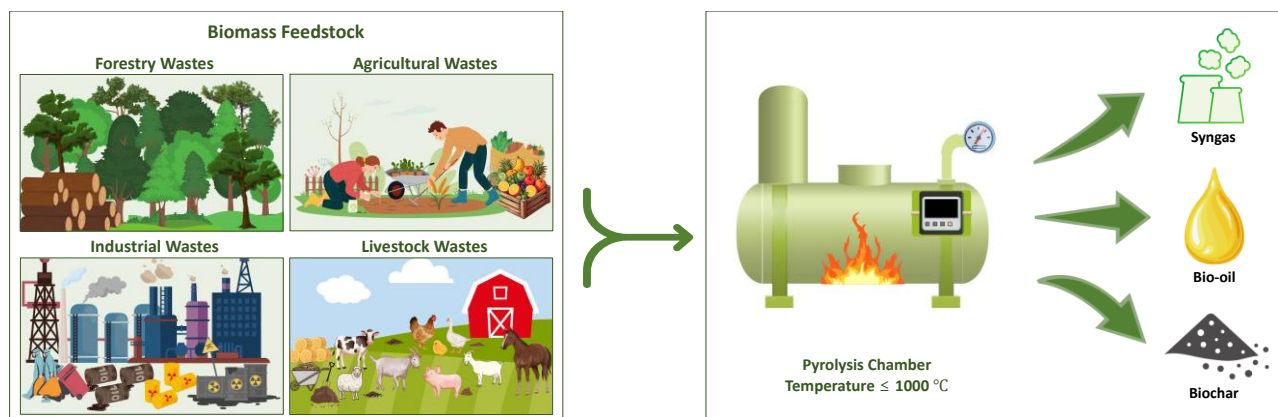
Sunflower husk	Silver Nanoparticles (AgNPs)	650 °C	AgNPs-Modified biochar	Tetracycline removal	42.04%	9.55 mg/g	[61]
Tea waste	Gold Nanoparticles (AuNPs)	500 °C for 2 h	biochar/Au Composite	Electrochemical sensor for nitrite detection	~ 100%	Not mentioned	[62]
White myoga ginger (W)	Gold Nanoparticles (AuNPs)	700, 850, and 950 °C for 2 h	W-biochar/Au	Detection of hydroquinone and catechol	~ 95-100%	Not mentioned	[63]
Wetland plant Reed	FeCl <sub>3</sub>	600 °C for 90 min	nZVIr-biochar	Removal of Pb <sup>2+</sup> , Cd <sup>2+</sup> , Cr <sup>6+</sup> , Cu <sup>2+</sup> , Ni <sup>2+</sup> , and Zn <sup>2+</sup> from polluted water sources	Pb <sup>2+</sup> , Cu <sup>2+</sup> , Cd <sup>2+</sup> , Ni <sup>2+</sup> , and Zn <sup>2+</sup> > 98% Cr <sup>6+</sup> = 48.9%	Pb <sup>2+</sup> = 38.31 mg/g Cu <sup>2+</sup> = 30.37 mg/g Cr <sup>6+</sup> = 23.09 mg/g Cd <sup>2+</sup> = 39.53 mg/g Ni <sup>2+</sup> = 47.85 mg/g	[64]
Pineapple peel waste	Fe <sub>2</sub> O <sub>3</sub> , Lanthanum Hydroxide (La(OH) <sub>3</sub> )	300 °C	Magnetic biochar with La(OH) <sub>3</sub>	Phosphate adsorption	> 96.04%	101.16 mg/g	[65]
Bark chips	Chitosan and nanoclay	600 °C at 10 °C/min and 2 h residence time under N <sub>2</sub> flow	Organic-inorganic composite of chitosan, nanoclay, and biochar	Immobilization of Cu, Pb, and Zn	MTCB reduces the metal leaching from the soil by 100, 100, and 52.29% for Cu <sup>2+</sup> , Zn <sup>2+</sup> , and Pb <sup>2+</sup> , respectively	Cu <sup>2+</sup> = 121.5 mg/g Pb <sup>2+</sup> = 336 mg/g Zn <sup>2+</sup> = 134.6 mg/g	[66]

Waste pinus needles ( <i>Pinus roxburghii</i> )	FeCl <sub>3</sub> /g-C <sub>3</sub> N <sub>4</sub> /FeVO <sub>4</sub>	600 °C at 10 °C/min	g-C <sub>3</sub> N <sub>4</sub> /FeVO <sub>4</sub> /Fe@NH <sub>2</sub> -biochar	Removal of methyl paraben (MeP) and 2-chlorophenol (2-CP)	98.4% degradation of MeP 90.7% degradation of 2-CP	Not mentioned	[74]
Sawdust	Ag/Fe Nanoparticles	500 °C	biochar-supported Ag/Fe nanoparticles (Ag/Fe/MB)	Removal of cephalexin from aqueous solution	More than 86% of CLX was removed by Ag/Fe/MB in 90 min	Not mentioned	[75]

1265

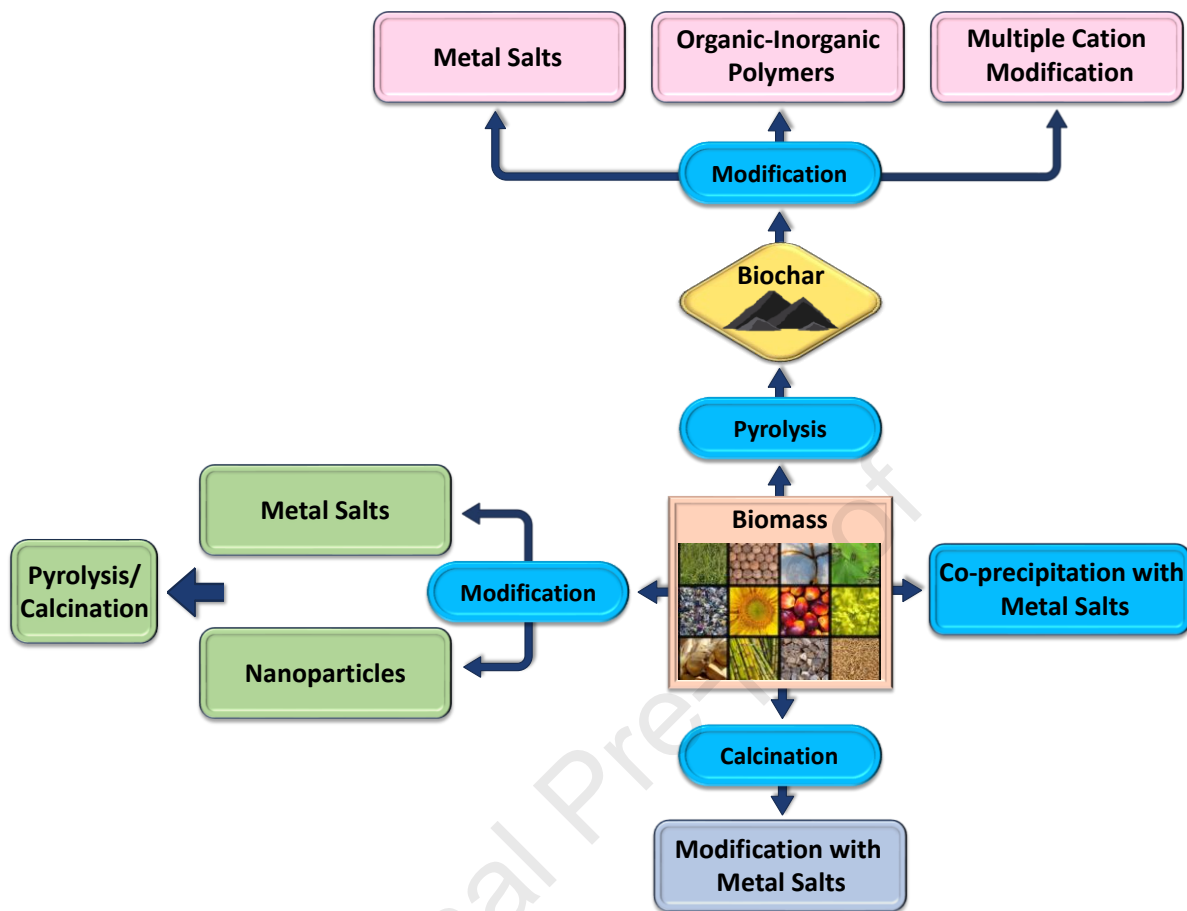
1266

1267



1268

1269 **Figure 1.** Feedstocks and pyrolytic outputs of biochar.

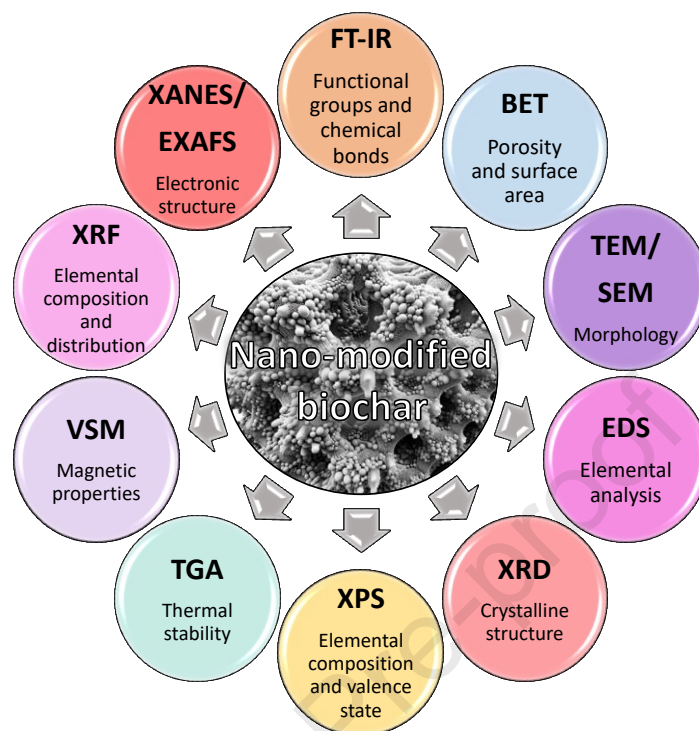


1270

1271 **Figure 2.** Schematic diagram of different modification techniques to prepare nano-modified

1272 biochar.

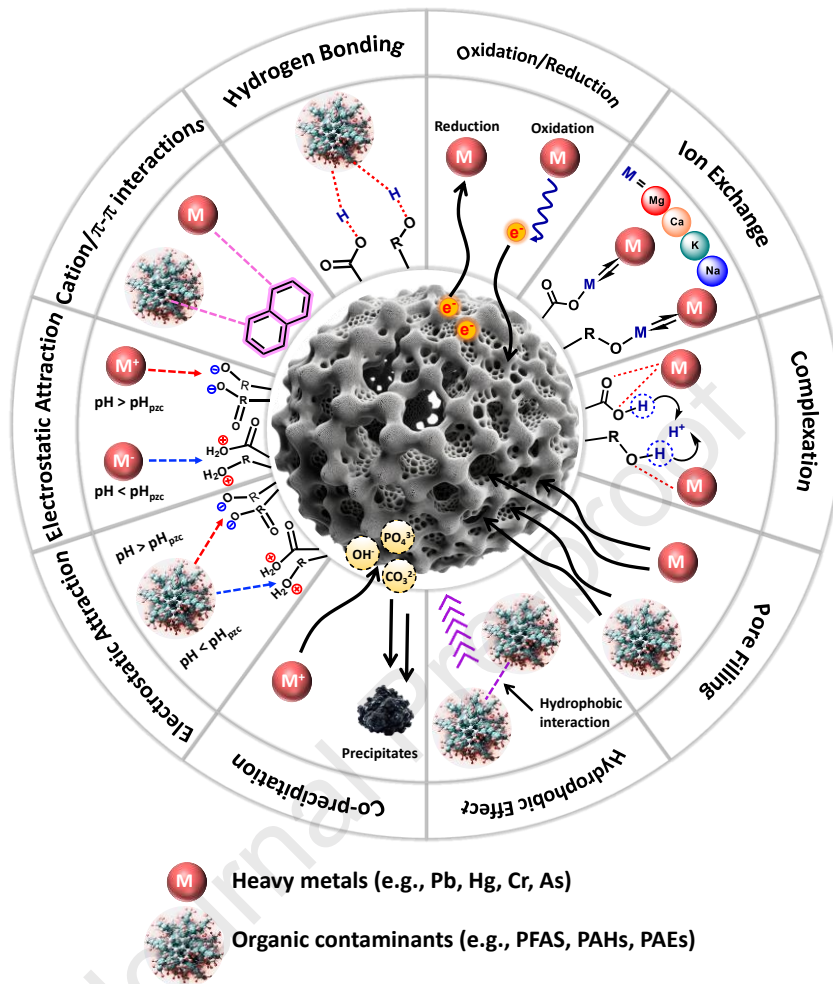
1273



1274

1275 **Figure 3.** Characterization techniques for nano-modified biochars. Fourier Transform Infrared  
 1276 Spectrometry (FT-IR), Brunauer–Emmett–Teller (BET) method, Transmission Electron  
 1277 Microscopy (TEM), Scanning Electron Microscopy (SEM), Energy-Dispersive X-ray  
 1278 Spectroscopy (EDS), X-ray Diffraction (XRD), X-ray Photoelectron Spectroscopy (XPS),  
 1279 Thermogravimetric Analysis (TGA), Vibrating Sample Magnetometer (VSM), Confocal Micro X-  
 1280 ray Fluorescence ( $\mu$ -XRF), X-ray Absorption Near-Edge Structure (XANES), and extended X-ray  
 1281 Absorption Fine Structure (EXAFS).

1282



1283

1284 **Figure 4.** Interaction mechanism between heavy metals and organic pollutants with biochar  
 1285 particles.

1286

1287

### **Highlights**

- The review provides a comprehensive summary of the preparation and synthesis techniques for nanomaterial-modified biochars.
- The review also details the characterization methods used for nanomaterial-modified biochars, highlighting how these techniques are crucial for understanding their structural and functional attributes.
- The review offers valuable insights into the use of biochar-supported metal nanoparticles (biochar-MNPs) for environmental remediation.
- The review discusses the underlying mechanisms by which nanomaterial-modified biochars effectively remove a wide range of contaminants.

**Declaration of interests**

The authors declare that they have no known competing financial interests or personal relationships that could have appeared to influence the work reported in this paper.

The authors declare the following financial interests/personal relationships which may be considered as potential competing interests:

Journal Pre-proof